Annu. Rev. Earth Planet. Sci. 2005. 33:335–67
doi: 10.1146/annurev.earth.33.092203.122505

First published online as a Review in Advance on January 21, 2005

EARTHQUAKE TRIGGERING BY STATIC, DYNAMIC, AND POSTSEISMIC STRESS TRANSFER

Andrew M. Freed
Department of Earth and Atmospheric Sciences, Purdue University, West Lafayette, Indiana 47907; email: freed@purdue.edu

Key Words Coulomb, aftershocks, earthquake-clusters, stress-shadows, viscoelastic

■ **Abstract** Earthquake triggering is the process by which stress changes associated with an earthquake can induce or retard seismic activity in the surrounding region or trigger other earthquakes at great distances. Calculations of static Coulomb stress changes associated with earthquake slip have proven to be a powerful tool in explaining many seismic observations, including aftershock distributions, earthquake sequences, and the quiescence of broad, normally active regions following large earthquakes. Delayed earthquake triggering, which can range from seconds to decades, can be explained by a variety of time-dependent stress transfer mechanisms, such as viscous relaxation, poroelastic rebound, or afterslip, or by reductions in fault friction, such as predicted by rate and state constitutive relations. Rapid remote triggering of earthquakes at great distances (from several fault lengths to 1000s of km) is best explained by the passage of transient (dynamic) seismic waves, which either immediately induce Coulomb-type failure or initiate a secondary mechanism that induces delayed triggering. The passage of seismic waves may also play a significant role in the triggering of near-field earthquakes.

INTRODUCTION

The 1990s saw a substantial and interesting sequence of earthquakes occur in the Mojave Desert of southern California in a region known as the Eastern California Shear Zone (ECSZ), which assists the San Andreas Fault system in accommodating North America/Pacific plate boundary motion (Savage et al. 1990). The earthquake sequence began in April 1992 with the $M_w = 6.1$ Joshua Tree earthquake, followed two months later by the June 1992 $M_w = 7.3$ Landers quake, which was followed by the $M_w = 6.3$ Big Bear earthquake by only 3 1/2 h (Hauksson et al. 1993). Seven years later, the October 1999 $M_w = 7.1$ Hector Mine earthquake (Dreger & Kaverina 2000) completed (to date) the sequence. As the average repeat time of faults within the ECSZ are of the order of thousands of years, this spatially and temporally closely spaced sequence is not likely coincidence, but rather the result of each earthquake being triggered by the previous events. We use the term trigger as a

reference to the initiation of a process that culminates in an earthquake that occurs after a time delay that may range from seconds to years after the causative event. Of course, differentiating triggered events from normal background seismicity is a key objective in studies of earthquake triggering.

Triggering occurs as a result of the redistribution of stress induced by an earthquake. Although earthquakes serve the overall function of relieving built-up elastic stress in the crust, stress in certain regions is actually increased by the occurrence of coseismic fault slip. If a fault lies in one of these regions of elevated stress, and is late in its own earthquake cycle, it is predisposed to being triggered. Triggering can happen very fast, such as the Big Bear earthquake following only hours after the Landers earthquake; after several years, such as the Hector Mine earthquake following seven years after Landers; or after several decades, such as the 1995 $M = 6.9$ Kobe, Japan earthquake, thought to have been triggering by the 1944 $M = 8.0$ Tonankai and the 1946 $M = 8.2$ Nankaido earthquakes (Pollitz & Sacks 1997). Understanding earthquake triggering has the potential to provide us with insight into the physics of the earthquake cycle and, most importantly, may greatly aid our ability to assess seismic hazards by pointing to where the next "domino" may fall in an earthquake sequence. For example, Parsons et al. (2000) use calculated stress changes associated with the 1999 $M_w = 7.4$ Izmit, Turkey earthquake and knowledge of 500 years of historic seismicity along the North Anatolian Fault to calculate a high probability ($62 \pm 15\%$) of a major earthquake occurring near Istanbul (population 10 million people) in the next 30 years.

Associated with the phenomenon of earthquake triggering is the related suppression of seismicity induced by large events. This is the case where shear loads on regional faults are reduced (or normal forces clamping those faults are increased) by a large nearby earthquake, thus delaying the time in which an earthquake would have been expected if one only considered the steady build-up of stress associated with regional tectonics. For example, the San Francisco Bay region experienced 14 $M_w \geq 6$ earthquakes in the 75 years leading up to the great 1906 San Francisco earthquake, yet only 2 in the 75 years after (Figure 1) (Bakun 1999). If this relatively quiescent period following the 1906 earthquake was due to the unloading of other Bay Area faults, the question remains as to how long such quiescence will last and whether events such as the 1989 Loma Prieta earthquake represent a new cycle of regional seismicity.

Earthquake triggering is also observed at distances much larger than a regional fault network. For example, the 1992 Landers earthquake triggered bursts of microseismicity as far away as Yellowstone National Park, more than 1250 km from the Landers epicenter (Hill et al. 1993), and the 2002 $M_w = 7.9$ Denali, Alaska earthquake triggered seismicity in the Coso geothermal field in southeastern California, more than 3600 km away (Prejean et al. 2004). Such distances challenge the notion that triggering is induced by the elastic stress changes associated with earthquake slip because at these distances such stress changes are far smaller than those caused even by lunar tides. Instead, triggering at such distances is commonly attributed to the effects of the passage of dynamic seismic waves that, although

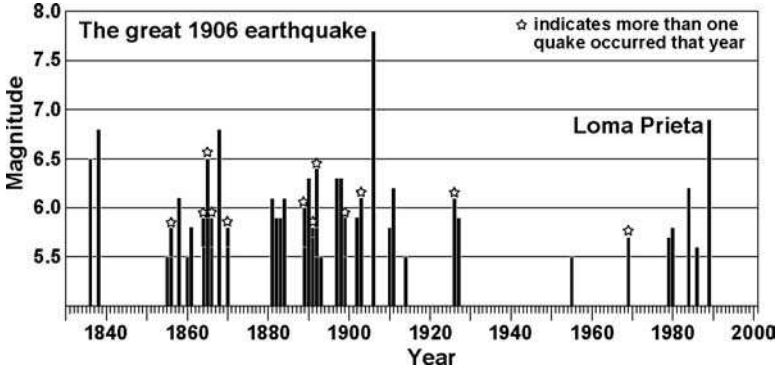

Figure 1 $M \geq 5.5$ earthquake activity in the San Francisco Bay region from 1836 through 1997 (after Bakun 1999).

transient, can be relatively large and either immediately trigger seismicity or initiate secondary mechanical processes that eventually lead to triggering. Of course, an affected fault has no idea how far the triggering dynamic stresses traveled to reach the fault, so it is just as likely that dynamic stresses associated with passing seismic waves influence local triggering as well. Understanding the relative influence of elastic (or static) stress changes relative to dynamic (or transient) stress changes, as well as the role of secondary mechanisms initiated by stress changes (such as viscous flow, fluid flow, and afterslip) represents a central focus of current research in earthquake triggering.

The key to understanding many triggering observations lies in calculated Coulomb stress changes. Here I review such calculations and their application to coseismic stress changes (also see reviews by King et al. 1994, Stein 1999, King & Cocco 2001, Stein 2003). I then review the latest work regarding postseismic stress-transfer mechanisms, which provide a means to explain long-term delayed triggering over large distances. Finally, I provide a comprehensive review of dynamic stress triggering, which appears to be the only process to transfer stresses quickly over great enough distances to trigger remote earthquakes. A related topic not covered here is seismicity triggered by man-made events, such as mining and reservoir development. A good review of these relationships has been conducted by Simpson (1986).

STATIC TRIGGERING

Coulomb Stress Changes

Earthquakes occur when the shear stresses that work to rupture a fault are large enough to overcome the normal (or clamping) stresses that, in combination with friction, prevent a locked fault from slipping. This balance can be characterized

by a Coulomb failure criterion (Jaeger & Cook 1979, Scholz 1990) for which a critical Coulomb failure stress, σ_c, is given by

$$\sigma_c = \tau - \mu(\sigma_n - p), \tag{1}$$

where τ is shear stress parallel to the slip direction, σ_n is normal stress, p is pore fluid pressure, and μ is the coefficient of friction. This equation implies that a fault can be brought closer to failure if the shear stress is increased or the effective normal stress (σ_n – p) is decreased (or vice versa).

The Coulomb failure criterion was developed in the laboratory where applied shear and normal stresses on rock specimens could be measured. In the field, stress magnitudes are difficult to measure and are poorly constrained. However, stress changes caused by an earthquake can be estimated, and from this estimate, one can calculate how the shear and normal stresses on neighboring faults are changed. Thus, although we may not know the absolute value of stress on a fault, we can calculate the change in Coulomb stress using the expression

$$\Delta\sigma_c = \Delta\tau - \mu(\Delta\sigma_n - \Delta p), \tag{2}$$

from which we can deduce whether a fault has been brought closer to (positive change in Coulomb stress) or further away from (negative change in Coulomb stress) an earthquake. Note that calculations are independent of any knowledge of the prevailing regional stresses or any preexisting stress fields from other events.

Pore fluid pressure changes are commonly assumed to be proportional to normal stress changes (see Cocco & Rice 2002) for an examination of this assumption) and incorporated into an effective coefficient of friction, μ', of the form

$$\mu' = \mu(1 - B), \tag{3}$$

where B is Skempton's coefficient, which rock experiments suggest typically ranges between 0.5 and 0.9 (e.g., Roeloffs 1996). The effective coefficient of friction in coseismic stress change studies has varied from 0.0 to 0.75, with an average value of $\mu' = 0.4$ often used. With this assumption, coseismic Coulomb stress changes take the form (Reasenberg & Simpson 1992)

$$\Delta\sigma_c = \Delta\tau - \mu'\Delta\sigma_n. \tag{4}$$

A coseismic Coulomb stress change calculation using Equation 4 is illustrated in Figure 2 (see color insert), where shear and normal stress changes owing to a right-lateral causative (or master) earthquake are calculated for similar oriented receiver faults in the surrounding region with a similar sense of slip (although the calculation can be performed for any fault orientation and slip). The summation of the shear and normal stress changes provides the Coulomb stress change. Regional faults that lie in areas of positive Coulomb stress change (warm colors) are brought closer to failure, whereas faults that lie in areas of negative Coulomb stress change (cool colors) are brought further away. Such calculations are referred to as static or elastic as they only consider elastic stress changes owing to

slip on an earthquake. Although limited in many respects, such as the inability to explain the time-dependence of triggered events, such calculations have proved successful in explaining a variety of seismic observations. An excellent review of static Coulomb stress change calculations can be found in King et al. (1994), which also discusses the determination of optimum slip planes for use in predicting aftershock distributions when the orientation of receiver faults is not known.

Aftershock Distributions

One of the key points to take away from Figure 2 is that Coulomb stress increases induced by an earthquake do not just occur at the fault tips, where the termination of slip leads to stress concentrations, but also in off-fault lobes. This is most clearly seen in the shear stress changes (left panel in Figure 2) and was cited by Das & Scholz (1981) as an explanation of why off-fault aftershocks were observed following the 1968 Borrego Mountain, California earthquake.

An example of off-fault aftershocks and their correspondence to calculated Coulomb stress increases is shown in Figure 3 (see color insert) for the 1979 M = 5.5 Homestead Valley, California earthquake. As typical for aftershock studies, the fit between calculated Coulomb stress increases and observed aftershocks is not perfect, with some aftershocks occurring in regions of Coulomb stress decrease. Regions of Coulomb stress decrease are known as stress shadows (Harris & Simpson 1996), as few aftershocks or triggering earthquakes should occur in such regions if the Coulomb hypothesis is valid. Generally, the best correlations of Coulomb stress change to aftershock distribution are at distances greater than a few kilometers from the fault. Closer to the fault, unknown details of the slip distribution and rupture geometry influence near-fault stress changes that are generally not accounted for in the Coulomb stress calculations.

Of particular note in Figure 3, and consistent with most triggering studies, is that the stress changes that lead to triggering are generally quite small. Most aftershock studies suggest that an increase of less than 0.1 to 0.3 MPa (1 to 3 bars) is generally sufficient to trigger seismicity, whereas reductions of the same amount can effectively suppress them (e.g., Stein & Lisowski 1983, Oppenheimer et al. 1988, Toda et al. 1998, Anderson & Johnson 1999). Such small magnitudes, which are only a small fraction of the stress drop that occurs during an earthquake, imply that the stress changes do not cause earthquakes, but only trigger them. Rydelek & Sacks (1999) modeled a fault as comprised of small patches that individually experience loading and failure, with failure resulting in the loading of neighboring patches, sometimes causing those patches to fail. In such models, earthquakes occur when failure on one patch leads to a chain reaction of many patches failing. Models like these show that as result of multiple (and repeated) failures over these small areas, faults can develop a very uneven stored stress state. Rydelek & Sacks (1999) show that with such heterogeneity, it is possible for small stress changes of only a few hundredths of a mega-Pascal to advance or retard the occurrence of large earthquakes by decades.

The assumed value for effective friction influences the contribution of normal stresses to the calculated Coulomb stress changes, and therefore the correspondence of Coulomb stress changes to aftershock distributions. Often, studies seek to find the effective coefficient of friction that leads to the best fit of aftershocks, using this technique to infer frictional strength. King et al. (1994) found the adjustments to friction had only modest effects on aftershock correlations and thus chose to use a median value of 0.4. Following the 1989 Loma Prieta, California earthquake, Parsons et al. (1999) found that high shear stress changes were correlated with seismicity-rate increases on major, high-angle, strike-slip faults, whereas high normal (unclamping) stress changes were significantly correlated with seismicity-rate increases on oblique (right-lateral/thrust) faults. The former implies a relatively low value of effective friction, whereas the latter implies a relative high value. Parson's et al. suggest that major strike-slip faults with large cumulative offset may have become impermeable through gouge build-up, thus trapping fluids and causing high pore-fluid pressures that negate imposed normal stress changes, whereas fluids can escape rapidly in faults with more limited offset, leading to a stronger influence of normal stress changes. This could further explain why intermediate coefficients of friction, such as the value used by King et al. (1994), may work well to describe the correspondence of Coulomb stress changes to aftershock distributions over broad regions that contain both types of faults.

Aftershock distributions have been well explained by coseismic Coulomb stress change calculations following the 1987 Elmore Ranch/Superstition Hills earthquake sequence (Anderson & Johnson 1999), the 1989 $M = 7.1$ Loma Prieta earthquake (Reasenberg & Simpson 1992, Parsons et al. 1999), the Landers earthquake (Hardebeck et al. 1998, Wyss & Wiemer 2000), the 1995 Kobe, Japan earthquake (Toda et al. 1998), and the 1983 $M = 6.5$ Coalinga and $M = 6.0$ Nuñez earthquakes (Toda & Stein 1998). These last events also decreased Coulomb stress on the locked segment of the San Andreas Fault to the south of Parkfield, potentially explaining (at least partially) why the 2004 $M = 6$ Parkfield earthquake occurred approximately two decades after it was expected based on the average repeat time of earthquakes on this segment (a review of the Parkfield experiment and prediction can be found at http://quake.wr.usgs.gov/research/parkfield/). Working the Coulomb/aftershock triggering problem backwards, Mueller et al. (2004) used the pattern of modern-day aftershocks to infer the most likely causative rupture surfaces associated with 1811–1812 New Madrid earthquakes.

Several studies suggest that Coulomb theory fails to explain other aftershock distributions: Only 60% of the aftershocks following the 1994 Northridge earthquake appear to lie in regions of Coulomb stress increase (Hardebeck et al. 1998); two faults that apparently lie in a stress shadow following the Chi-Chi, Taiwan earthquake had significant aftershock activity (Wang & Chen 2001); Marsan (2003) observed that quiescence in stress shadows was seldom observed for timescales beyond 100 days following the Loma Prieta, Landers, and Northridge earthquakes; Mallman & Zoback (2003) found that following the Landers and Kobe earthquakes, seismicity rates went up everywhere; and Felzer & Brodsky (2003) found no

significant correlation between the amount of observed seismicity rate decrease and distance from the rupture surface of the Landers earthquake, suggesting that the earthquake sequence did not produce a stress shadow.

The occurrence of a few aftershocks in a region of calculated Coulomb stress decrease could arise from oversimplifications of modeled fault slip, unaccounted for heterogeneities of crustal properties, or the existence of small faults with azimuthal orientations different from that of the prevailing fabric. However, the general lack of a stress shadow as inferred by some studies (e.g., Felzer & Brodsky 2003, Mallman & Zoback 2003) may be indicative of the failure of Coulomb theory. A potential problem with statistical studies of the existence of stress shadows, however, is that background seismicity prior to an earthquake is usually too sparse to provide a statistically significant sample from which to infer postseismic rate decreases.

Several studies have addressed the significance of background seismicity by utilizing increased seismicity rates following an earthquake as the background seismicity for a second nearby event. Toda & Stein (2003) utilize the 1997 Kagoshima, Japan couplet to show that a region of significant aftershock activity associated with the first event became a region of decreased activity associated with a Coulomb stress decrease following the second event (Figure 4, see color insert). A separate study has shown that certain regions of aftershock activity induced by the 1992 Landers quake were turned off by negative Coulomb stress changes associated with the 1999 Hector Mine earthquake (S. Toda, R. Stein, K. Richards-Dinger, S. Bozkurt, submitted manuscript). Both of these studies conclude that stress shadows can be observed if the background seismicity prior to an earthquake is significant.

In each of these earthquake sequence studies the authors found that although observing seismicity associated with a sequence confirmed the influence of Coulomb stress changes, simply adding the stress changes did not explain the time-dependence of the ensuing seismicity, such as the rate change, the temporal decay, and the migration of seismicity away from the rupture ends. Toda & Stein (2003) and Toda et al. (S.Toda, R. Stein, K. Richards-Dinger, S. Bozkurt, submitted manuscript) therefore implemented a stress transfer model that incorporated rate and state friction. Rate and state friction is the name of a constitutive relation based on laboratory observations in which friction on a fault is a function of time, slip, and slip velocity (Dieterich 1979, 1981). Here "rate" refers to the rate at which the fault slips and "state" refers to the physical properties of the fault surface or gouge (Dieterich 1994, Scholtz 1998). As formulated by Ruina (1983),

$$\mu(t) = \mu_o + a\ \ln[V(t)/V_o] + b\ \ln[\xi(t)V_o/d_c], \tag{5}$$

where μ is friction, t is time, μ_o is a reference frictional coefficient, V is the rate at which the fault slips, V_o is a reference velocity, d_c represents a critical slip distance associated with the evolution of contact points along the fault surface, a and b are dimensionless coefficients determined from laboratory experiments, and $\xi(t)$ represents the physical state of the contact surface or gouge and evolves according to

$$d\xi(t)/dt = 1 - \xi(t)V(t)/d_c, \quad (6)$$

which requires that the fault strengthens when stationary or slipping slowly and weakens when slipping rapidly relative to the regional velocity field. A thorough review of rate and state friction laws and their application to faulting can be found in Marone (1998).

Because of the logarithmic dependence of friction on rate and state, a sudden increase in load on the fault, even of very small amplitude, can rapidly reduce fault friction and bring about an acceleration to failure (Gomberg 1998). The earlier in the earthquake cycle that a fault is stressed by a nearby earthquake, the more the fault is advanced in its own earthquake cycle. Thus, rate and state friction predicts that the sudden stressing of a population of faults, in which the time of each fault's earthquake cycle is randomly distributed, will lead to a clustering of triggered seismicity (e.g., Gomberg 1998) that obeys the observed Omori aftershock decay law (Dieterich 1994). Such theory has also been used to convert calculated Coulomb stress changes into time-dependent probability forecasts for triggered seismicity (Stein et al. 1997; Toda et al. 1998; Toda & Stein 2002, 2003; Parsons et al. 2000). Toda & Stein (2003) and Toda et al. (S.Toda, R. Stein, K. Richards-Dinger, S. Bozkurt, submitted manuscript) use a stress transfer model and rate and state in which seismicity is treated as a sequence of independent nucleation events that are dependent on the fault slip, slip rate, and elapsed time since the last event. Their models of earthquake sequences reproduce (although imperfectly) the temporal response of seismicity to successive stress changes, including toggling of aftershock activity, aftershock decay rates, and the migration of aftershocks away from rupture ends.

Earthquake Triggering Sequences

The success of Coulomb stress changes to explain aftershock distributions contradicts the long-held theory that earthquakes strike randomly. Subsequently, Coulomb stress changes have been used to explain the aforementioned Joshua Tree-Landers-Big Bear-Hector Mine sequence (Figure 5, see color insert) (see also King & Cocco 2001) and a variety of other sequences. For example, the 1933 M = 6.4 Long Beach and 1952 M = 7.3 Kern County, California earthquakes combined to increase Coulomb stress at the eventual hypocenter of the 1971 M = 6.7 San Fernando earthquake, which in turn Coulomb loaded the eventual hypocenter of the 1994 M = 6.7 Northridge earthquake (Stein et al. 1994). At least six of seven earthquakes that occurred in a sequence between 1888 and 1994 east of the Alpine fault in New Zealand occurred in regions of Coulomb stress caused by the previous events (Doser & Robinson 2002). For earthquakes in northwest Turkey and the north Aegean Sea since 1912, four times as many events occurred in regions in which Coulomb stresses were increased by previous events (Nalbant et al. 1998). An earthquake sequence in the Rainbow Mountain-Fairview Peak-Dixie Valley, Nevada was preceded by a Coulomb stress increase from prior events (Hodgkinson

et al. 1996), and Nostro et al. (1997) found that earthquake triggering associated with Coulomb stress increases also worked to explain the 1980 Irpinia normal faulting sequence.

In a broader study, Deng & Sykes (1997a) calculated the evolution of Coulomb stress in southern California since 1812, using seven $M \geq 7$ earthquakes and tectonic loads from plate motions, and found that 95% of the well-located $M \geq 6$ earthquakes with mechanisms involving either strike-slip or reverse faulting are consistent with Coulomb theory (i.e., occurred in regions of Coulomb stress increase). This study was extended by Deng & Sykes (1997b) to conclude that more than 85% of the $M \geq 5$ earthquakes from 1932 to 1995 occurred in regions of positive Coulomb stress change, with the remaining 15% having uncertainty owing to lying close to the boundary between positive and negative Coulomb stress changes.

In a study of the triggering of the 1954 $M_s = 6.8$ Dixie Valley earthquake less than 5 min after the $M_s = 7.2$ Fairview Peak earthquake in Central Nevada, Caskey & Wesnousky (1997) observed something not often reported in triggering studies. Detailed study of the Fairview Peak surface rupture, which consisted of sequential rupture along four distinct faults, showed a correlation between the largest surface offsets and the magnitude of positive Coulomb stress change owing to the rupture of the previous segments. Caskey & Wesnousky suggest that this observation, combined with a correspondence between the location of rupture termination and a change in the sign of Coulomb stress, implies that Coulomb stress-changes provided more than just a trigger, but actually influenced the slip distribution and extent of the triggered segments.

One of the primary reasons to study earthquake triggering is to work toward being able to predict where the next seismic event will occur. In a study of a 60-year sequence of earthquakes along the North Anatolian Fault in Turkey, Stein et al. (1997) found that all but one event was promoted by the previous events. Based on these calculations and historic events in the region, Stein et al. (1997) suggested an elevated risk for a major shock along two sections of the North Anatolian Fault, one of which ruptured in August 1999, the $M = 7.4$ Izmit earthquake. Cumulative changes in Coulomb stress are calculated to have evolved over the past 60 years to load the Izmit region, not only explaining the triggering of the Izmit earthquake but also the distribution of seismicity in the region from 1993 to just before the 1999 earthquake (Parsons et al. 2000). The Izmit earthquake in turn elevated Coulomb stresses at the site of the $M = 7.1$ Düzce earthquake, which occurred just 3 months later (Parsons et al. 2000). Together, the Izmit and Düzce earthquakes killed 18,000 people. According to Parsons et al., the trigger is poised to be pulled on Istanbul, an urban center of 10 million people. Parsons et al. suggest there is a $62 \pm 15\%$ probability of strong shaking in the Istanbul region in the next 30 years and $32 \pm 12\%$ probability in the next decade.

Earthquake triggering is also evident in subduction zone dynamics. Lin & Stein (2004) show that large interplate-subduction zone earthquakes promote normal faulting events in the outer rise, and thrust faulting events on the periphery

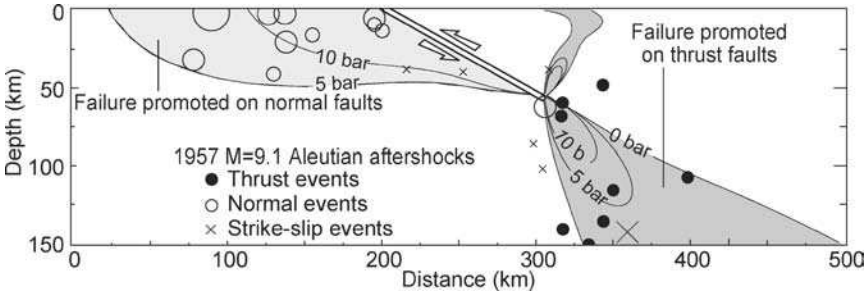

Figure 6 Composite figure showing Coulomb stress changes imparted to normal faults in the outer rise and Coulomb stress changes imparted to thrust faults in the downdip region following the 1957 $M_w = 9.1$ Aleutian interplate earthquake. Also shown are aftershocks associated with this earthquake. (From Lin & Stein 2004.)

of the seismic rupture and on its downdip extension. Figure 6 shows a good correspondence between Coulomb stress changes and the location and type of aftershocks following the 1957 $M_w = 9.1$ Aleutian interplate earthquake. Similar studies have also shown that subduction-zone earthquakes have been promoted by preceding events and have in turn triggered subsequent events, including aftershocks (e.g., Dmowska et al. 1988; Taylor et al. 1996, 1998; Parsons 2002). Lin & Stein (2004) also examined stress changes associated with the 1960 $M_w = 9.5$ and 1995 $M_w = 8.1$ Chile earthquakes and found that Coulomb stress increases of 0.2 to 2.0 MPa corresponded closely to sites of aftershocks and postseismic slip, whereas aftershocks were absent where Coulomb stress decreases were more than 1 MPa (see also a discussion of continental thrust events in Lin & Stein 2004).

Similar to aftershock studies, verifying that large stress shadows cast by great earthquakes diminish moderate and large earthquakes throughout a region is one of the best means to test the Coulomb hypothesis. Two of the biggest and best observed stress shadows were cast by the great 1857 Fort Tejon and great 1906 San Francisco earthquakes (Harris & Simpson 1998). Figure 7 shows calculated Coulomb stress changes (for similarly oriented strike-slip faults and low friction) for both earthquakes superimposed on a single map of California (similar calculations have been accomplished for the triggering of reverse faults following the Fort Tejon earthquake showing that thrust faults in the Transverse Ranges and Los Angeles Basin were put under a stress shadow as well). The stress shadow cast by the Fort Tejon earthquake halted the occurrence of $M > 6$ earthquakes throughout the shadow region (which also includes the ECSZ) for 50 years following the great earthquake (Ellsworth 1990, Harris & Simpson 1996). Of 13 $M \geq 5.5$ earthquakes to occur in the southern California region between 1857 and 1907, at least 11 (although possibly all 13) occurred in regions in which Coulomb stress was increased by the Fort Tejon earthquake. The correlation disappears around 1907, suggesting to Harris & Simpson (1996) that tectonic loading began to overwhelm

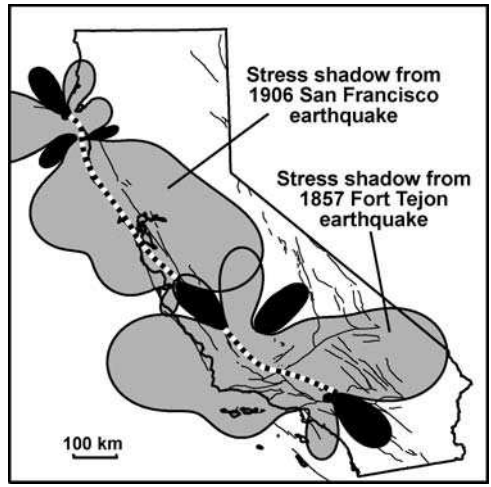

Figure 7 Composite of calculated Coulomb stress changes (*black*: positive, *gray*: negative) owing to the 1857 Fort Tejon and 1906 San Francisco earthquakes. Calculations based on right-lateral strike-slip faults with an azimuth of N35°W and $\mu' = 0.4$. The increase and decrease regions are ≥ 0.01 and ≤ -0.01 MPa, respectively (combined from figures from Harris & Simpson 1998).

the effect of the 1857 earthquake in the early twentieth century. As shown in Figure 1, the cessation of earthquake activity in the San Francisco Bay region following the 1906 earthquake was dramatic (see also Ellsworth 1990). In terms of seismic moment release, the rate in the 56 years before 1906 is approximately 10 times that in the 70 years after 1906 (Bakun 1999). Jaumé & Sykes (1996) found that the rate of activity in the San Francisco Bay region did not just decrease following the 1906 earthquake but also following a large event in 1868 and the 1989 M = 6.9 Loma Prieta earthquake (see also Reasenberg & Simpson 1992).

In a survey of several global earthquake catalogs, Kagan & Jackson (1991) found that long-term clustering, not periodicity, characterized the occurrence of all earthquakes—shallow, intermediate, and deep. Although Kagan & Jackson suggest that clustering is due to dynamic processes in Earth's mantle, this could also be a reflection of the significance of earthquake triggering working to synchronize faults within a fault system. In a broad study of earthquake triggering using a global earthquake catalog, Parsons (2002) calculated shear stress changes induced by earthquakes with $M_s \geq 7$ on subsequent rupture planes near enough to be potentially triggered. Parsons found that 61% of earthquakes near enough to incur a shear stress change of ± 0.01 MPa were associated with shear stress increases, whereas 39% were associated with shear stress decreases. If earthquakes associated with calculated shear stress increases are interpreted as triggered, then 8% of the global catalog can be considered triggered events. Parsons could not calculate

Coulomb stress change because of difficulties associated with identifying correct nodal planes (required for the determination of normal stress changes) in a global study and required estimations of poorly constrained effective friction. It is thus unknown how the statistics of the study would change if it were possible to calculate Coulomb stress changes. Nevertheless, this broad study demonstrates the correspondence of at least one of the stress components to triggering of earthquakes on a global scale.

POSTSEISMIC STRESS TRANSFER AND STRENGTH WEAKENING

Postseismic Stress Transfer Mechanisms

How the 1992 Landers earthquake triggered the 1999 Hector Mine earthquake is difficult to explain not only because of the seven-year delay time, but also because it was not obvious that the Landers earthquake induced a coseismic Coulomb stress increase at the Hector Mine hypocenter. Calculations found the Hector Mine hypocenter to be very close to a boundary between positive and negative Coulomb stress changes (near the lobe of positive Coulomb stress change to the northeast of Landers in Figure 5*b*). Therefore, modest changes in modeling assumptions or the location of the hypocenter (which is not definitively known) greatly influence the sign of the modeled stress change (e.g., Harris & Simpson 2002). Despite these uncertainties, the Hector Mine hypocenter occurred in a region that experienced one of the highest seismicity rate increases following the Landers earthquake (Wyss & Weimer 2000). Thus, the Hector Mine earthquake could potentially have been triggered by intervening aftershocks. Felzer et al. (2002) note that the Hector Mine earthquake was preceded by the M = 5.4 Pisgah aftershock, which occurred approximately 4 km from the eventual Hector Mine epicenter, as well as M = 4.3 and M = 4.1 aftershocks that occurred within 2 km of the epicenter. In fact, Felzer et al. (2003) argues that more than 50% of aftershocks are triggered by other aftershocks.

Another possible explanation of the seven-year delay time between events would be if the Coulomb stress changes associated with the Landers earthquake continued to evolve such that significant change in stress at the Hector Mine hypocenter occurred years after the Landers event. One mechanism that induces significant postseismic change in the stress field is that of viscous relaxation of a warm lower crust or upper mantle. At depths below approximately 15 km, high pressures and temperatures prevent rock from failing in a brittle manner; instead, they flow viscously in response to stress (e.g., Kirby & Kronenberg 1987). Earthquakes occur so rapidly, however, that even these viscous regions respond to coseismic stresses by elastic deformation. However, following the earthquake these regions begin to relax and the stored elastic strains are transferred upward to the seismogenic upper crust, leading to increased stresses in the upper crust. For

vertical strike-slip faults, regions of positive coseismic Coulomb stress change tend to increase in magnitude owing to viscous relaxation, and regions in which coseismic stress changes were negative tend to get more negative. For thrust and normal faulting events, the redistribution of stress is generally of the opposite sense, where coseismic stress increases and stress shadows tend to be reversed by the relaxation process (Freed & Lin 1998, Nostro et al. 2001).

In the Landers-Hector Mine sequence, calculations of postseismic stress transfer owing to viscous relaxation suggest a moderate to significant build-up of stress at the Hector Mine hypocenter in the seven years following the Landers earthquake (Freed & Lin 2001, Zeng 2001, Pollitz & Sacks 2002). Figure 8*a* (see color insert) shows the calculated coseismic change in Coulomb stress associated with the Landers earthquake resolved on the Hector Mine rupture surface. These results show that the Hector Mine hypocenter was located near a narrow strip of slightly positive Coulomb stress changes bounded by regions of negative stress changes to the north and south. Of particular interest is the large lobe of positive coseismic Coulomb stress changes induced in the lower crust and upper mantle by the Landers earthquake. If a warm and viscously weak lower crust and upper mantle is unable to support these stresses, they will migrate to the upper crust. Such a process has been calculated to have increased Coulomb stress at the Hector Mine hypocenter (Figure 8*b*), potentially explaining the triggering of the earthquake. Postseismic stress changes may have also influenced the extent of the Hector Mine earthquake, as the spatial extent of the rupture zone appears to coincide with stress changes solely owing to postseismic relaxation (Figure 8*c*).

The Mojave earthquake sequence lies perilously close to the San Bernardino Mountain segment of the San Andreas Fault. This segment is located only 80 km from Los Angeles, is capable of $M > 7$ earthquakes and has not ruptured since 1812; historic repeat times suggest that this segment may be late in its earthquake cycle (Sieh 1989). The Joshua Tree/Landers/Big Bear earthquakes were calculated to have brought this segment closer to failure by increasing Coulomb stress (Stein et al. 1992, Jaumé & Sykes 1992). Subsequent to 1992, the process of stress transfer owing to viscous relaxation, the occurrence of the Hector Mine earthquake, and continued relaxation processes are calculated to have further increased stress on this segment, and will continue to increase stress for years to come (Freed & Lin 2002). This segment of the San Andreas Fault may therefore be a good candidate for a major earthquake in Southern California in the near future.

Stress transfer between faults through viscous relaxation may be a general cause of earthquake clustering. For example, Lynch et al. (2003) suggest that seismicity on a northern and southern San Andreas–type fault system (large stick-slip faults separated by a creeping section) can become coupled by the transfer of stress through lower crustal flow. Chéry et al. (2001) appeals to a similar stress transfer process to explain a sequence of three $M > 8$ earthquakes that occurred in Mongolia during a 52-year period despite great distances (400 km) that separate the events. And in a global review of the relative distance and time delay separating pairs of earthquakes, Marsan & Bean (2003) found that seismic activity diffuses

away from an earthquake as the delay time increases following its occurrence, which they attributed to viscous diffusion of stress in the upper mantle. Viscous relaxation can also induce the opposite effect: retard seismicity in a region. For example, Casarotti & Piersanti (2003) show that the viscoelastic relaxation of asthenosphere following major earthquakes that occurred in the past 60 years along the South American arc decreased Coulomb stress, thus inducing two seismic gaps (regions in which earthquake are overdue based on historical repeat times) near southern Peru and north Chile.

The reach of stress transfer by postseismic relaxation of a viscous lithosphere can extend great distances from the mainshock source. Stress loading from postseismic relaxation of oceanic asthenosphere following a 1952 to 1965 sequence of large earthquakes along the Aleutian arc and Kurile-Kamchatca plate boundary was found to be consistent with the triggering of oceanic intraplate earthquakes, temporal patterns in seismicity at remote plate boundaries, and geodetic measurements of anomalous velocities over a 7000 by 7000 km^2 area during the 30 years following the sequence (Pollitz et al. 1998). Viscous processes can also serve to facilitate stress interactions between faults over larger spans of time. For example, viscoelastic relaxation following the 1944 M = 8.0 Tonankai and the 1946 M = 8.2 Nankaido, Japan earthquakes has been shown to have slowly reduced clamping stresses on the Nojima Fault, inducing the 1995 M = 6.9 Kobe earthquake (Pollitz & Sacks 1997). Similarly, postseismic stress changes from asthenospheric relaxation were shown to be an important component of the markedly increased seismicity in the decades following the 1891 M = 8 Nobi, Japan earthquake and worked to prevent the expected (based on the historic record) extension of the 1944 Tonankai earthquake into the Suruga Trough (Pollitz & Sacks 1995). Viscous processes may also play a role in aftershock distributions, as Melosh (1976) appeals to a non-Newtonian viscous asthenosphere to explain seaward migration of aftershocks following the 1965 Rat Island, Alaska earthquake.

Viscous relaxation is not the only means of redistributing stress following an earthquake. Poroelastic rebound occurs when coseismic stresses produce significant excess fluid pressure in the near-field region, the decay of which always fluids to "rebound" to their pre-quake state, potentially inducing significant postseismic deformation and stress changes. Peltzer et al. (1998) suggest that poroelastic effects played a prominent role in near-fault postseismic deformations following the 1992 Landers earthquake. Masterlark & Wang (2002) use a poroelastic upper crust coupled to a viscoelastic lower crust to explain transient postseismic deformations following the Landers earthquake and a redistribution of stress that loaded the Hector Mine hypocenter, potentially aiding the triggering of the Hector Mine earthquake.

A third mechanism considered to be a potentially important contributor to postseismic stress transfer is afterslip. Afterslip is the process by which unrelieved stress on the fault induces aseismic slip after the earthquake within the rupture surface, or deeper regions of the fault that generally slip aseismically because of high pressures at depth. Afterslip, whether shallow or deep, can lead to an

increase in stress in certain regions of the upper crust, potentially loading nearby faults. Afterslip has been inferred to be the primary mechanism of postseismic deformation following the 1999 $M_w = 7.5$ Izmit, Turkey earthquake, leading to a further loading of the eventual hypocenter of Düzce earthquake which followed by only 87 days (Hearn et al. 2002).

DYNAMIC TRIGGERING

Observations of Remotely Triggered Seismicity

Within minutes after the 1992 Landers earthquake, seismic activity increased at widely scattered locations across the western United States at distances outside the aftershock zone (i.e., greater than 1–2 fault lengths) up to and beyond 1000 km from the Landers epicenter (Hill et al. 1993, Anderson et al. 1994). This seismicity included swarms of earthquakes along the boundary of the Basin and Range and the Sierra Nevada (Nevada/California border) up to 650 km from the Landers epicenter, the Geysers thermal area of northern California (750 km away), the southern Cascade range in northern California (900 km away), western Idaho (1100 km away), and as far away as Yellowstone National Park (more than 1250 km away) (Hill et al. 1993). Most of these remotely triggered events were small ($M = 1$ to 3), but several $M > 4$ events were triggered, including a $M_s = 5.6$ earthquake at Little Skull Mountain in southern Nevada (240 km from Landers) that followed the Landers earthquake by 22 h (Anderson et al. 1994, Gomberg & Bodin 1994), and is believed to be the largest earthquake to occur in southern Basin and Range since 1868 (Hill et al. 1993).

Much of the remotely triggered seismicity following the Landers earthquake occurred either in conjunction with or within a few minutes of the passage of the seismic waves induced by the Landers rupture, although triggered seismicity persisted from between hours to weeks, with an average delay time (time between the causative and triggered events) of approximately a day (Hill et al. 1993, Anderson et al. 1994). Although these observations strongly support a causative relationship between the Landers rupture and increased seismicity throughout the western United States, it is most convincing to confirm the inference of triggered seismicity by comparing the seismicity rates before and after the Landers earthquake. One way to do this is by simply plotting the cumulative number of earthquakes to occur at trigger sites throughout 1992, as accomplished by Hill et al. (1993) and shown in Figure 9. Cumulative earthquakes show a dramatic increase throughout the western United States associated with the occurrence of the Landers earthquake (day 180). Anderson et al. (1994) estimated that approximately 10% of the potentially triggered events would have occurred in any randomly selected time interval, or that 90% of the recorded events were triggered by the Landers earthquake. Gomberg et al. (2001) used a β-statistic sensitive to the contrast of average seismicity rate between two time intervals (Mathews & Reasenberg 1988) to demonstrate seismicity-rate changes following the Landers earthquake. This

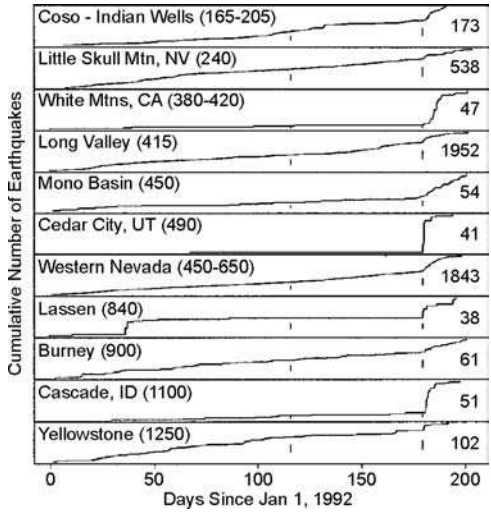

Figure 9 Cumulative number of locatable earthquakes in selected zones, beginning January 1, 1992. Numbers in parentheses are distances (in kilometers) from the Landers epicenter. Total number of earthquakes in each zone is shown at right. Vertical lines mark times of the M = 7.1 Petrolia (Cape Mendocino) and M = 7.3 Landers earthquakes. (From Hill et al. 1993.)

result is shown in Figure 10 (see color insert), where a β-statistic greater than 2.0 is suggestive of a significant average rate increase.

Remote triggering following the Landers earthquake raised the question of whether this was an unusual event or just the first major earthquake to occur in a region so densely covered with seismic stations that ample remotely triggered small events could be detected. As pointed out by Hill et al. (1993), before the late 1970s many of the present networks were sparse or nonexistent. There have been four post-1980 earthquakes of M = 6.9 or greater that occurred in the western United States that did not trigger significant recorded remote seismicity. These events include the 1980 M = 7.4 Eureka, California (which is essentially the same seismic moment as Landers earthquake); the 1983 M = 6.9 Bora Peak, Idaho; the 1989 M = 7.1 Loma Prieta, California; and the 1992 M = 7.1 Petrolia, California earthquakes (note the lack of remote triggering by the Petrolia earthquake at day 116 in Figure 9).

Although the Loma Prieta and Petrolia earthquakes did not trigger widespread remote seismicity, they did trigger microearthquake swarms (M = 2 or less events) at the Geysers geothermal region in northern California's Coast Ranges (Stark & Davis 1996). This highly active region, which experiences small earthquakes on the average of 40 to 50 per day, seems to be particularly sensitive to being triggered by distant large events. Aside from the Loma Prieta (210 km away), the Petrolia (220 km away), and the Landers (750 km away) earthquakes,

microearthquakes at the Geysers were also triggered by two 1991 events (M_s = 6.9 and M_s = 7.1) on the Gorda Plate (445 km and 400 km away, respectively); the 1994 M_s = 6.6 Northridge earthquake (635 km); and most illuminating, the 1988 M_s = 7.6 Gulf of Alaska earthquake, which was approximately 2500 km away (Stark & Davis 1996). (The phenomenon of triggering at the Geysers by remote events was not recognized earlier because seismic data at the Geysers was not made available to Stark & Davis from private industry until well after the Landers earthquake.)

Evidence of remotely triggered earthquakes was again observed following the 1999 M_w = 7.1 Hector Mine earthquake. Although not nearly as dramatic in scale as remotely triggered seismicity following the larger Landers earthquake, Hector Mine induced an increase in seismicity throughout southern California and into northern Mexico many fault lengths from the epicenter (Gomberg et al. 2001). Triggered seismicity from Hector Mine included two moderate M = 4.7 and M = 4.4 earthquakes near the Salton sea, triggered 30 s and 10 min, respectively, after the passage of seismic waves (Hough & Kanamori 2002) and events in Baja California, Mexico, 260 km away (Glowacka et al. 2002). Remote triggering was also observed following the 2000 M = 7.4 Izmit, Turkey earthquake, where widespread seismicity was triggered in Greece at distances of 400 to 1000 km away (Brodsky et al. 2000), and after a 1995 M_s = 7.3 Gulf of Aqaba earthquake, which triggered a swarm of seismic activity within the Dead Sea Fault system more than 500 km away (Mohamad et al. 2000).

Motivated by observations of remote triggering following the Landers earthquake, earthquake catalogs have been searched for evidence of remote triggering associated with historic seismicity. Singh et al. (1998) surveyed catalogs of historic subduction zone earthquakes along the Pacific coast of Mexico since 1920 and found at least nine coastal events, which may have triggered increases of seismicity in the Valley of Mexico, which is situated at least 250 km away. Hough (2001) and Hough et al. (2003) used the distribution of felt reports and qualitative descriptions of ground motions to infer potentially triggered earthquakes following the 1811–1812 New Madrid and the 1886 Charleston, South Carolina earthquakes. Remote seismicity is inferred to have followed within seconds to days after the passage of surface waves of these events at distances exceeding 500 km, such as in Northern Kentucky following one of the Missouri earthquakes and in Connecticut following the South Carolina earthquake. Meltzner & Wald (2003) used existing catalogs and historical documents to infer remote triggered earthquakes following the 1906 San Francisco, California earthquake. They found that within 2 days of the San Francisco earthquake, events were potentially triggered in southern California, western Nevada, and southern Oregon at distances that range from 350 to 670 km from San Francisco, and perhaps a triggered event in western Arizona more than 800 km away.

The most spectacular evidence of large-scale remote triggering after the Landers earthquake came from the 2002 M = 7.9 Denali, Alaska earthquake. The 340-km-long Denali rupture was the largest strike-slip earthquake to occur in North America

in almost 150 years, causing ground shaking felt as far as 3500 km away and large lake oscillations that rocked boats in Louisiana (Eberhart-Phillips et al. 2003). The Denali earthquake also triggered remote seismicity throughout western North America, ranging from British Columbia to southern California (Figure 11) (Eberhart-Phillips et al. 2003, Gomberg et al. 2004, Prejean et al. 2004, Pankow et al. 2004). Triggered seismicity included events at Mount Rainer in central Washington, the Coso and Geysers geothermal fields and Mammoth Mountain and Long Valley Caldera in California (Prejean et al. 2004), Yellowstone (Husen et al. 2004), and throughout most of Utah's main seismic belt (Pankow et al. 2004). The triggered seismicity in Utah occurred along the Wasatch Fault zone that bisects Utah and is particularly interesting in that this region did not show a strong seismic response to the Landers earthquake, which was located more than 1000 km closer. In most regions, triggered seismicity following the Denali earthquake began immediately with the passage of seismic waves and lasted from between several minutes to several days (Eberhart-Phillips et al. 2003, Gomberg et al. 2004, Prejean et al. 2004). Triggered events in Utah following the Denali earthquake began almost

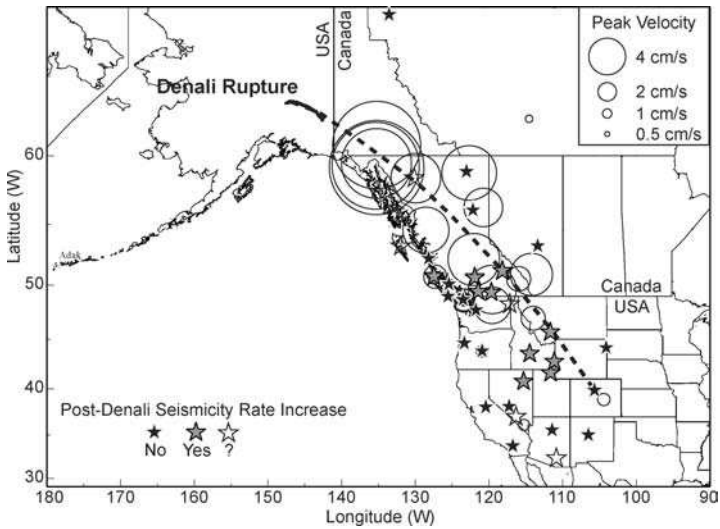

Figure 11 Map of the distribution of Denali-related seismicity rate changes and measured peak Denali seismic ground velocities. The latter are proportional to the dynamic strains at these distances. Circle centers show locations of recording sites with radii proportional to the measured peak velocity (scale in inset). The velocities decrease away from the direction of theoretically expected maximum seismic radiation (*dashed line segment of a great circle*). Notably, the sites of triggered rate increases lie roughly within the same azimuthal span as is defined by the maximum measured velocities and theoretically expected dynamic deformations. (From Gomberg et al. 2004.)

immediately after the passage of surface waves, remained intense for the first 24 h, then took 25 days to decay back to background level (Pankow et al. 1993).

In an interesting contrast to the shallow events, it is worth mentioning that dynamic triggering is also observed in association with deep-focus earthquakes. Deep focus earthquakes (e.g., Green & Houston 1995) occur at depths of 400–700 km, challenging prevailing ideas of how earthquakes occur, as brittle failure is not expected to occur in the deep mantle where high temperatures and pressures make rock more likely to flow viscously rather than fracture. Deep earthquakes have characteristics that are distinct from shallow earthquakes (e.g., Weins 2001), such as larger stress drops, variations in magnitude-frequency relations, fewer aftershocks, and of particular interest, the lack of surface waves commonly cited as important in the dynamic triggering of shallow events. Yet, Tibi et al. (2003) describe a 598-km-deep, $M_w = 7.6$ earthquake near Tonga in 2002 that triggered, 7 min later, a 664-km-deep, $M_w = 7.7$ earthquake more than 300 km away. This is approximately a distance of 10 fault lengths, more than far enough to categorize this event as a remotely triggered. Interestingly, the triggered event here occurred in the opposite direction of rupture directivity of the initial event, suggesting that preexisting conditions may play a more important role in deep earthquake triggering than rupture directivity. In addition to the 2002 Tonga sequence, Tibi et al. (2003) surveyed catalogues of deep earthquakes and found several other remotely triggered sequences. This includes a 1986 Tonga sequence where a $M_w = 6.8$ at 590 km depth triggered a $M_w = 7.1$ earthquake at 543 km depth at an estimated 30 to 40 fault lengths.

Stress Transfer by Dynamic Seismic Waves

The great distance of triggered seismicity by the Landers earthquake was a watershed event in two ways. First, it had not been widely observed or recognized that earthquakes could trigger seismicity at more than a few fault lengths. Second, at these distances (Yellowstone was 17 fault lengths away from Landers) static Coulomb stress changes are calculated to be so small that they ought not be significant enough to trigger an earthquake. The magnitude of static stress changes fall-off between r^{-1} and r^{-2}, where r is the distance from the fault (Cotton & Coutant 1997). Coseismic Coulomb stress changes following the Landers earthquake are calculated to drop below daily lunar tidal stress change magnitudes ($\sim$0.003 MPa) at a distance of 200 km, and a tenth of tidal stresses at a distance of approximately 500 km (Hill et al. 1993). In contrast, peak transient stresses associated with passing seismic waves fall-off at a rate of less than r^{-1} (Cotton & Coutant 1997). Pankow et al. (2004) estimate peak dynamic stresses in Utah following the 3000 km distant Denali earthquake ranged from 0.12 to 0.35 MPa, a couple of orders of magnitude greater than tidal stresses despite the great distance. Thus, the passage of dynamic seismic waves seems to be a more plausible means by which to transmit stress changes rapidly over great distances, albeit such changes are transitory.

The hypothesis that transient seismic waves are a key component of dynamic triggering can be tested by comparing the distribution of triggered seismicity following an earthquake to the rupture's directivity, the direction in which a rupture propagates during an earthquake. Seismic energy is focused in the rupture direction, which in turn causes the highest velocities and therefore dynamic stresses along the azimuth of directivity. If the dynamic stresses are greatest in this direction, and if dynamic stresses are a key mechanism of dynamic triggering, then seismicity rates following the earthquake should be greatest in line with the directivity (Gomberg et al. 2003). This was found to be the case of triggering following the Landers earthquake at both near and remote distances, which ruptured from south to north (Wald & Heaton 1994). Hill et al. (1993) calculated that peak dynamic stresses to the north-northwest of Landers were approximately twice those at comparable distances to the west and more than three times the magnitude of dynamic stresses to the south. As shown in Figure 10, the Landers earthquake induced a dramatic increase in seismicity rates to the north-northwest of the Landers rupture, strongly indicating that transient dynamic stresses play an integral role in remote triggering (Hill et al. 1993, Anderson et al. 1994, Gomberg et al. 2001). Gomberg et al. (2003) also observed this correlation between the rupture direction and greatest rate increases in the near-field (i.e., aftershock zone) for a number of clearly directive earthquakes globally.

The importance of rupture directivity was verified by the 1999 Hector Mine earthquake and again in a spectacular fashion by the 2002 Denali rupture. In the Hector Mine case, the fault ruptured primarily from north to south [although some segments ruptured south to north (Dreger & Kaverina 2000)], and it appears to have triggered a strong seismic response to the south as far as Mexico (Gomberg et al. 2001). The 2002 Denali earthquake ruptured from the northwest to the southeast, toward the western United States (Eberhart-Phillips et al. 2003). The energy flux of teleseismic surface waves recorded at North American stations, in line with the Denali rupture directivity, was four to five times greater than the energy recorded at European and Asian stations at the same distance in the back-azimuth direction (Eberhart-Phillips et al. 2003). Consistent with predictions for dynamic stress triggering, Figure 11 shows that triggered events following the Denali earthquake follow in a fairly continuous band that lies in the direction of Denali directivity (Gomberg et al. 2004).

If dynamic stresses associated with seismic waves are responsible for triggering remote seismicity, then the question arises of what characteristics of the wave train are important to the triggering process. Gomberg (1996) used broadband seismic data at various triggered and nontriggered sites following the Landers earthquake to infer that if a critical triggering amplitude threshold exists, it varies from site to site. In support of this observation, Brodsky et al. (2000) found that the amplitude of dynamic stresses required to trigger earthquakes in Greece following the Izmit earthquake were at least a factor of three lower than the threshold inferred for triggering of Imperial Valley seismicity following the Landers earthquake. And Gomberg et al. (2004) found that despite the clear relationship between rupture

directivity and triggering seismicity following the Denali earthquake, there is not a one-to-one correspondence between the peak amplitude of the dynamic deformation (or stress) and the change in seismicity rate.

A particularly useful study of dynamic triggering thresholds was conducted by Brodsky & Prejean (2004) based on triggered seismicity at the Long Valley Caldera. Similar to the Geysers region, faults within Long Valley show susceptibility to being triggering by large remote earthquakes, but unlike the Geysers region, Long Valley experiences many cases of strong shaking that do not induce triggering. This makes Long Valley an ideal location to investigate which characteristic of the passing seismic waves is responsible of for triggering seismicity. Brodsky & Prejean find that observed triggering by seismic waves is inconsistent with any mechanism that depends on cumulative shaking or the peak amplitude of shaking. As shown in Figure 12, passing seismic waves associated with the 1994 Northridge earthquake contained larger horizontal and vertical peak amplitude velocities than seismic waves associated with the Denali earthquake, although the Northridge earthquake did not induce triggered seismicity at Long Valley, whereas the Denali earthquake did. Brodsky & Prejean found triggering at Long Valley to be best explained by a frequency-dependent triggering threshold, where long-period

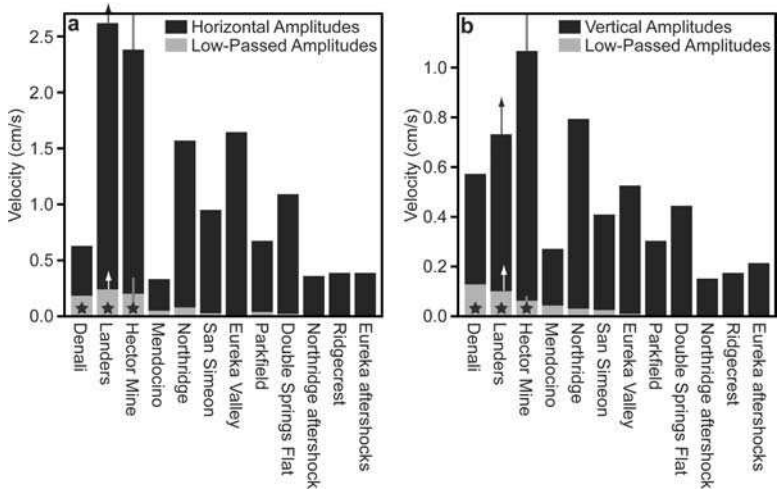

Figure 12 Peak amplitudes of (*a*) horizontal and (*b*) vertical seismograms recorded in Long Valley Caldera for triggering (*starred*) and non-triggering earthquakes. Low-pass amplitudes show the peak amplitudes of the seismic records after they have been low-pass filtered at 30 s. Earthquakes are listed in descending order of magnitude. Arrows indicate lower bounds for Landers. Error bars for Hector Mine are based on the corrections for using a different seismometer site (top error bar is truncated). The upper bound for the unfiltered Hector Mine shaking is 6.4 cm/s on the horizontal and 1.8 cm/s on the vertical. (From Brodsky & Prejean 2004.)

waves (>30 s) are more effective at generating local seismicity than short-period waves of comparable amplitude. Brodsky & Prejean cite the persistence of long-period surface waves to penetrate to greater depths than high-frequency waves as a contributing factor in their efficacy in triggering earthquakes. These results are in contrast with those of Gomberg & Davis (1996), who suggested that high-frequency waves were more effective at triggering.

Near-Field Dynamic Triggering

Several authors suggest that if dynamic stresses are strong enough to trigger earthquakes at distances out to several hundred kilometers, there is no reason why such stresses should not trigger aftershocks or earthquakes at distances comparable to a single fault length or less. That is, the affected fault has no knowledge of the distance to the source of the dynamic load, so the distinction between remote and local is purely one of observational capabilities. At remote distances, the contribution of dynamic static stresses becomes larger than static stress changes, and thus it is easier to associate rate changes with them. If dynamic stresses are responsible for aftershocks, Kilb et al. (2000, 2002) suggest that increased seismicity rates should correlate with regions of peak transient stresses. They test this hypothesis by calculating transient stresses associated with the Landers earthquake and converting these into peak dynamic Coulomb stresses, which are plotted in Figure 13 (see color insert). The peak transient stress changes display a very asymmetric pattern compared to the static stresses (Figure 5*b*), owing to the effects of rupture directivity (south to north). A comparison of the seismicity rate change following the Landers earthquake (Figure 10) shows a clear relationship between peak dynamic Coulomb stresses and the asymmetry of the seismic rate change.

Gomberg et al. (2003) conduct a broader study of near-field dynamic triggering by comparing aftershock distributions to rupture directivity following more than a dozen earthquakes worldwide. Of nine earthquakes with unilateral rupture, they find that eight produced greater near-field seismicity rate increases in the rupture direction. Because rupture directivity should affect only dynamic deformations, this result is consistent with the hypothesis that dynamic stresses play a significant role in the distribution of aftershocks within a fault length. In a related study, Kilb et al. (2002b) suggests that large peak dynamic stresses following the Landers earthquake could have played a role in the eventual triggering of the Hector Mine earthquake.

Several studies have shown that dynamic transfer of stress enables fault propagation during an earthquake to jump across unbroken spans of up to 5 km between fault segments (e.g., Harris et al. 1991, 2002; Kase & Kuge 1998). Voisin et al. (2000) suggest that dynamic stress transfer may explain both the triggering and 20 s time delay (arising from a slip-dependent friction law) of a jump to a subevent following the 1980 Irpinia, Italy earthquake. The 2002 Denali earthquake experienced a jump from the previously unrecognized Susitna Glacier thrust fault, where the sequence initiated, to the strike-slip Denali fault (Eberhart-Phillips et al. 2003).

This raised speculation that an earthquake initiating on the Sierra Madre–Cucamonga thrust fault system on the edge of Los Angeles could potentially dynamically trigger a rupture on the strike-slip San Andreas or San Jacinto faults (Anderson et al. 2003). Although a dynamic stress analysis by Anderson et al. (2003) suggests that such a triggering scenario is unlikely, they do find that an earthquake on the northern San Jacinto Fault could dynamically trigger a cascading rupture on the Sierra Madre-Cucamonga system, potentially causing a M_w = 7.5 to 7.8 earthquake on the edge of the Los Angeles metropolitan region.

The Tectonics of Regions Susceptible to Dynamic Triggering

Following the Landers earthquake, dynamically triggered seismicity was generally observed to occur in regions of previous seismic activity (Hill et al. 1993, Anderson et al. 1994), suggesting that triggering may generally occur in fault systems that are critically stressed. For example, significant post-Landers activity occurred in a belt of persistent seismicity and Holocene faulting in the border region between the Basin and Range and the Sierra Nevada. Similarly, triggered swarms in southwestern Utah occurred along the active Hurricane Fault zone that bounds the Colorado Plateau and the eastern Basin and Range (Hill et al. 1993). Most of the triggered volcanic regions, such as the Long Valley Caldera, are noted for a long history of seismic activity (Hill et al. 1995). In contrast, however, the 1999 Izmit earthquake triggered remote seismicity in a region of normally low seismic activity (Brodsky et al. 2000), and three of seven clusters of triggered seismicity in Utah following the 2002 Denali earthquake occurred in regions with little or no prior seismicity (Pankow et al. 2004). Also, Gomberg et al. (2004) suggest that triggered seismicity following the Denali earthquake occurred in areas not obviously tectonically active, for example, in the foothills of the Canadian Cordillera in south-central British Columbia, at the edge of a province that is considered to be ancient stable North America. These observations lead Gomberg et al. to suggest that faults may be critically stressed everywhere (e.g., Townend & Zoback 2000), making earthquake triggering a "ubiquitous and unpredictable" process.

It is also important to note that several regions noted for their persistent seismicity did not experience significant triggering by the Landers earthquake, such as active sections of the San Andreas Fault system in central and northern California. Gomberg (1996) suggests that the spatial variations of Landers-triggered seismicity may be a consequence of the characteristics of the San Andreas system versus the less active faults of the ECSZ. For example, the more mature and active San Andreas system potentially has a thicker and more deformed fault gouge that requires greater stress changes to induce rupture. Alternately, Gomberg (1996) suggests that thicker fault gouge within the San Andreas system may have enabled dynamic strains to be accommodated by aseismic slip that could have gone undetected, although such slip has been observed following more than a dozen southern California earthquakes (Bodin et al. 1994). Most interestingly, the Borrego Mountain earthquake triggered aseismic slip on the San Andreas Fault

in a region where static Coulomb stress changes were calculated to be negative (Allen et al. 1972).

Hill et al. (1993) noted that many of the triggered regions following the Landers earthquake were closely associated with geothermal activity or were near recent (past one million years) volcanic activity. Examples include the Long Valley Caldera, the Geysers geothermal area in northern California, and Coso Hot Springs. However, Anderson et al. (1994) pointed out that although most of the major active volcanoes in the region had some level of triggered activity following Landers, only a small fraction of the triggered events correlate with volcanism, suggesting that such provinces are not a necessary requirement for dynamic triggering. This is confirmed by observations of dynamic triggering in nonvolcanic regions of Greece following the Izmit, Turkey earthquake (Brodsky et al. 2000); in Ohio after the 1811–1812 New Madrid earthquakes (Hough 2001); and in Syria following the 1995 Gulf of Aqaba earthquake (Mohamad et al. 2000). On the other hand, Anderson et al. (1994) note that most of the triggered regions to the north of Landers have potential geothermal resources, perhaps providing a necessary if not sufficient condition for dynamic triggering, as not all geothermal regions experience seismicity increases. This may be consistent with Brodsky et al. (2000), who suggest that geothermal activity may be a common characteristic of dynamic triggering in Greece following the 1999 Izmit, Turkey earthquake because hot springs occur over much of that region. Future observations of remote triggering should help to clarify the tectonics of triggering susceptible regions.

Mechanisms for Dynamic Triggering

One obvious problem with triggering owing to seismic waves is that despite the fact that dynamic stresses may be large, they are transient, leaving no permanent change to the stress state once the waves pass. Thus, dynamic stresses should only be able to trigger seismicity by Coulomb failure as the wave train passes. Although immediate events have been detected following the Landers (Hill et al. 1993), Denali (Prejean et al. 2004), and Izmit (Brodsky et al. 2000) earthquakes, most remote-triggered seismicity occurs after a delay period between seconds to weeks. This implies that either dynamic stresses must initiate a time-dependent acceleration to failure process, such as that described by rate-and-state friction, or a secondary mechanism that leads to a delayed rupture, such as one involving a transient increase in pore pressure.

In addition to rate and state friction, another accelerating failure process is subcritical crack growth. In subcritical crack growth, small cracks within a fault zone grow slowly in response to accelerated chemical reactions between silicate rocks and water (Atkinson 1984). The rate of crack growth is proportional to the intensity of stress at the crack tips, which in turn is proportional to crack size. A sudden transfer of stress to the rock will cause the size of cracks to become larger, thus increasing stress intensities and acceleration in crack growth, leading to a delayed fault failure.

To explore whether a fault controlled by an accelerating failure process has the potential of being triggered by dynamic stresses, Gomberg et al. (1997, 1998) developed heuristic spring-slider analytical models. These models explore the idea of clock advance in which the time that a fault would have failed owing to simple, continuous background loading is advanced by the additional loading associated with dynamic stresses. Although oversimplified, the spring-slider system employed by Gomberg et al. (1997, 1998) is physically analogous to a fault patch undergoing stick-slip behavior. Such models suggest that when a fault is loaded by dynamic stresses, the amount of clock advance increases the later in the earthquake cycle in which the loading occurs. Thus, if a population of faults at varying times within their individual earthquake cycles are perturbed by a dynamic load, the faults later in their cycle will experience more clock advance than those earlier in the cycle (Gomberg 1997). This will induce a seismicity rate decrease as the time to failure diverges for the population, in contrast to observed seismicity rate increases following earthquakes. Thus, at least with respect to rate-and-state friction and subcritical crack growth mechanisms, transient dynamic stresses can not explain delay triggering.

This conclusion is also consistent with Scholz (1998), who suggests that the direct effect of friction (the sudden increase in friction caused by a sudden change in slip velocity) and the finite size and duration of nucleation prohibit earthquakes from being triggered by high-frequency stress oscillations, such as those generated by passing seismic waves. It is also consistent with another spring-slider study. Belardinelli et al. (2003) found that although a static stress change is able to advance as well as delay an induced instability depending on its sign, a dynamic stress pulse is able to promote a nearly instantaneous failure, but not induce delayed triggering. Brodsky & Prejean (2004) also suggest that the frequency-dependent threshold inferred from triggered Long Valley seismicity is not consistent with a rate-and-state friction law or subcritical crack growth, as each of these mechanisms are sensitive to an amplitude, as opposed to a frequency, threshold.

An alternative class of mechanisms considers processes that, when initiated by oscillatory stresses associated with seismic waves, lead to a time-dependent increase in pore pressure, which lead to an effective decrease in effective normal (clamping) stresses. Once effective normal stresses drop below an unknown threshold level, triggered rupture is initiated. For example, Hill et al. (1993) suggest that the interaction of the dilatational component of compressional waves with fluids in the crust could alternately raise and lower local pore pressure, inducing almost instantaneous faulting; or such stresses could rupture fluid seals within the fault, allowing subsequent fluid flow to increase pore pressure. In the latter case, the delay time of triggered seismicity would be governed by local permeability, ambient pore pressures, and shear stresses.

In support of the ruptured seal scenario, Brodsky et al. (2003) note that dynamic stresses associated with remote earthquakes several thousand miles away induced large, sustained well-water level changes in Oregon, indicating significant pore pressure changes. Distant earthquakes, including the 1989 Loma Prieta, 1992

Landers, and 1999 Hector Mine earthquakes, have also induced ground-water level changes persisting for days to weeks at Long Valley Caldera, California (Roeloffs et al. 2003). Brodsky & Prejean (2004) envision a hydrological system in which constant precipitation and material transport can temporarily block fractures and cause isolated pockets of heterogeneous pore pressure. The seismic waves serve to unclog these fractures, allowing the pore pressure to reequilibrate and induce an effective pressure increase. They suggest that a fracture unclogging mechanism would be consistent with triggering observations at the Long Valley Caldera that suggest a threshold sensitive to low-frequency seismic waves. Roeloffs et al. (2003) suggest that water level changes at the Long Valley Caldera may be related to the upward movement of magma or hot aqueous fluid based on borehole strain data that showed seismic wave–induced strain-rate changes, which on some occasions lasted for many days after the causative event.

Sturtevant et al. (1996) suggest that rectified diffusion, a process by which the vapor density of bubbles in hydrothermal or magmatic systems increases owing to seismic oscillations, can induce pore pressure increases. Vapor density increases because oscillations drive a cyclic process of bubble expansion and contraction, and more mass diffuses into the bubbles during the expanding phases, causing a net increase in pore pressure. Sturtevant et al. suggest that this process may have produced pressure changes significant enough to have induced triggered seismicity at the Long Valley Caldera following the Landers earthquake. Furthermore, percolation may serve to continue to increase pore pressure in hydrothermal and magmatic systems over timescales much longer than the duration of the remote earthquake, thus leading to delayed triggering.

Linde et al. (1994) suggest that triggering at the Long Valley Caldera may have been induced by advective overpressure, which could occur if gas bubbles were shaken loose inside the magma chamber then proceeding to rise. The rising bubbles could have caused pressure inside the magma body to increase as pressures at the level of the rising bubbles equilibrated to the higher pressure consistent with that of the bubbles' origin. One difficulty with this mechanism is that it takes a finite amount of time for a bubble to rise and induce advective overpressure. Such a mechanism could therefore not readily explain seismicity that occurs during the passage of the wave train or soon after. Another potential mechanism related to the disturbance of magma involves seismic waves rupturing isolated compartments containing superhydrostatic fluid pressures, inducing a hydraulic pressure surge at shallower depths and thereby weakening caldera faults (Johnston et al. 1995). Of course, all magma-related mechanisms require the presence of magma, which is not the case for a significant portion of remotely triggered sites.

SUMMARY

Although simplistic in many respects, calculations of static Coulomb stress changes associated with earthquake slip have proven to be a powerful tool for explaining many seismic observations. Such calculations have been successful in explaining

aftershock distributions and the location of triggered earthquakes as occurring in regions of stress increase at the edges of a ruptured fault and at off-fault lobes of stress increase. Many sequences of large earthquakes have been successfully explained in such a fashion. Coulomb stress decreases have also been shown to coincide with regions of minimal aftershock activity and the seismic quiescence of broad, normally active regions following large earthquakes, such as the San Francisco Bay Area following the 1906 earthquake and southern California following the 1857 Fort Tejon earthquake. Although several studies suggest that stress shadows do not exist, it seems more likely that earthquakes occur in regions of calculated stress shadows because of modeling oversimplifications or because most aftershock studies draw upon a paucity of prequake aftershocks from which to draw statistical conclusions. The toggling of seismicity associated with the 1997 Kagoshima, Japan couplet and the Landers-Hector Mine earthquake sequence, appear to validate Coulomb theory, although much more testing needs to be accomplished.

Calculations of coseismic Coulomb stress changes combined with rate and state friction laws appear to explain both spatial and temporal observations of aftershocks, but not necessarily longer (year to decade) delay times between causative and triggered earthquakes. Studies suggest that longer duration delayed triggering could be induced by mechanisms that redistribute stress postseismically, such as viscoelastic relaxation, poroelastic rebound, or afterslip. Postseismic viscoelastic relaxation, in particular, provides a means by which to explain earthquake clusters that occur across large distances and over many decades.

Remotely triggered seismicity that occurs at distances greater than 1–2 fault lengths appears to be a common occurrence after very large earthquakes. It is most likely the result of the passage of transient seismic waves that provide a means of transmitting large stresses to great distances with great speed. Strong evidence of dynamic triggering lies in the association between the distribution of triggered seismicity and rupture directivity. Although more easily recognized at remote distances, the same underlying physical mechanisms must also operate in the near field, raising the question of the relative contribution of these mechanisms to aftershock distributions. More observations of remotely triggered seismicity are required to determine whether dynamic triggering is confined to geothermal or volcanic regions. Because they leave no permanent stress changes, it is not obvious how transient dynamic stress changes associated with seismic waves induce fault failure. Studies suggest that secondary mechanisms associated with pore pressure increases are a likely candidate.

ACKNOWLEDGMENTS

I wish to thank Joan Gomberg, Emily Brodsky, and Karen Felzer for helpful reviews. I also wish to thank Ross Stein for his enormous efforts in bringing the concepts and implications of earthquake triggering research to both scientific and public communities. His work, along with that of Jian Lin, has inspired my own research.

LITERATURE CITED

Allen CR, Wyss M, Brune JN, Granz A, Wallace R. 1972. Displacements on the Imperial, Superstition Hills, and San Andreas faults triggered by the Borrego Mountain earthquake. In *The Borrego Mountain Earthquake*, 787:87–104. U.S. Geol. Surv. Prof. Pap. Reston, VA: U.S. Geol. Surv.

Anderson G, Aagaard B, Hudnut K. 2003. Fault interactions and large complex earthquakes in the Los Angeles area. *Science* 302:1946–49

Anderson G, Johnson H. 1999. A new statistical test for static stress triggering: application to the 1987 Superstition Hills earthquake sequence. *J. Geophys. Res.* 104:20153–68

Anderson JG, Brune JN, Louie JN, Zeng YH, Savage M, et al. 1994. Seismicity in the western Great Basin apparently triggered by the Landers, California, earthquake 28 June 1992. *Bull. Seismol. Soc. Am.* 84:863–91

Atkinson BK. 1984. Subcritical crack growth in geologic materials. *J. Geophys. Res.* 89: 4077–114

Belardinelli ME, Bizzarri A, Cocco M. 2003. Earthquake triggering by static and dynamic stress changes. *J. Geophys. Res.* doi: 108:10.1029/2002JB001779

Bodin P, Bilham R, Behr J, Gomberg J, Hudnut KW. 1994. Slip triggered on southern California faults by the 1992 Joshua Tree, Landers, and Big Bear earthquakes. *Bull. Seismol. Soc. Am*. 84:806–16

Brodsky EE, Karakostas V, Kanamori H. 2000. A new observation of dynamically triggered regional seismicity: earthquakes in Greece following the August, 1999 Izmit, Turkey earthquake. *Geophys. Res. Lett.* 27:2741–44

Brodsky EE, Prejean SG. 2004. New constraints on mechanisms of remotely triggered seismicity from Long Valley Caldera. *J. Geophys. Res*. In press

Brodsky EE, Roeloffs E, Woodcock D, Gall I, Manga M. 2003. A mechanism for sustained groundwater pressure changes induced by distant earthquakes *J. Geophys. Res.* doi: 108:10.1029/2002JB002321

Casarotti E, Piersanti A. 2003. Postseismic stress diffusion in Chile and South Peru. *Earth Planet. Sci. Lett.* 206:325–33

Caskey SJ, Wesnousky SG. 1997. Static stress changes and earthquake triggering during the 1954 Fairview Peak and Dixie Valley earthquakes, central Nevada. *Bull. Seismol. Soc. Am.* 87:521–27

Chery J, Carretier S, Ritz JF. 2001. Postseismic stress transfer explains time clustering of large earthquakes in Mongolia. *Earth Planet. Sci. Lett.* 194:277–86

Cocco M, Rice JR. 2002. Pore pressure and poroelasticity effects in Coulomb stress analysis of earthquake interactions. *J. Geophys. Res.* doi: 107:10.1029/2000JB000138

Cotton F, Coutant O. 1997. Dynamic stress variations due to shear faults in a plane-layered medium. *Geophys. J. Int.* 128:676–88

Das S, Scholz CH. 1981. Off-fault aftershock clusters caused by shear stress increase? *Bull. Seismol. Soc. Am.* 71:1669–75

Deng J, Sykes LR. 1997a. Evolution of the stress field in southern California and triggering of moderate-size earthquakes: a 200-year perspective. *J. Geophys. Res.* 102:9859–86

Deng J, Sykes LR. 1997b. Stress evolution in southern California and triggering of moderate-, small-, and micro-size earthquakes. *J. Geophys. Res.* 102:24411–35

Dieterich JH. 1979. Modeling of rock friction: 1. Experimental results and constitutive equations. *J. Geophys. Res.* 84:2161–68

Dieterich JH. 1981. Constitutive properties of faults with simulated gouge. In *Mechanical Behavior of Crustal Rocks*. *Geophys. Monogr. Ser.* 24:103–20. Washington, DC: Am. Geophys. Union

Dieterich JH. 1994. A constitutive law for rate and of earthquake production and its application to earthquake clustering. *J. Geophys. Res.* 99:2601–18

Dmowska R, Rice JR, Lovison LC, Josell DJ. 1988. Stress transfer and seismic phenomena in coupled subduction zones during the earthquake cycle. *J. Geophys. Res.* 93:7869–84

Doser DI, Robinson R. 2002. Modeling stress changes induced by earthquakes in the southern Marlborough region, South Island, New Zealand. *Bull. Seismol. Soc. Am.* 92:3229–38

Dreger DS, Kaverina A. 2000. Seismic remote sensing for the earthquake source process and near-source strong shaking; a case study of the October 16, 1999 Hector Mine earthquake. *Geophys. Res. Lett.* 27:1941–44

Eberhart-Phillips D, Haeussler PJ, Freymueller JT, Frankel AD, Rubin CM, et al. 2003. The 2002 Denali fault earthquake, Alaska: a large magnitude, slip-partitioning event. *Science* 300:1113–18

Ellsworth W. 1990. Earthquake history, 1769–1989. In *The San Andreas Fault System, California*, ed. R Wallace, 1515:153–88. U.S. Geol. Surv. Prof. Pap. Reston, VA: U.S. Geol. Surv.

Felzer KR, Abercrombie RE, Ekström G. 2003. Secondary aftershocks and their importance for aftershock forecasting. *Bull. Seismol. Soc. Am.* 93:1433–48

Felzer KR, Becker TW, Abercrombie RE, Ekström G, Rice JR. 2002. Triggering of the 1999 M_w 7.1 Hector Mine earthquake by aftershocks of the 1992 Mw 7.3 Landers earthquake. *J. Geophys. Res.* doi:107: 10.1029/2001JB000911

Felzer KR, Brodsky EE. 2003. The absence of stress shadows. *Seismol. Res. Lett.* 75:285

Freed AM, Lin J. 1998. Time-dependent changes in failure stresses following thrust earthquakes. *J. Geophys. Res.* 103:24393–409

Freed AM, Lin J. 2001. Delayed triggering of the 1999 Hector Mine earthquake by viscoelastic stress transfer. *Nature* 411:180–83

Freed AM, Lin J. 2002. Accelerated stress buildup on the southern San Andreas Fault and surrounding regions caused by Mojave Desert earthquakes. *Geology* 30:571–74

Glowacka E, Nava FA, de Cossio GD, Wong V, Farafan F. 2002. Fault slip, seismicity, and deformation in Mexicalli Valley, Baja California, Mexico, after the M 7.1 1999 Hector Mine earthquake. *Bull. Seismol. Soc. Am.* 92:1290–99

Gomberg J. 1996. Stress/strain changes and triggered seismicity following the M_w 7.3 Landers, California earthquake. *J. Geophys. Res.* 101:751–64

Gomberg J. 2001. The failure of earthquake failure models. *J. Geophys. Res.* 106:16253–63

Gomberg J, Beeler NM, Blanpied ML. 1998. Earthquake triggering by transient and static deformations. *J. Geophys. Res.* 103:24411–26

Gomberg J, Blanpied ML, Beeler NM. 1997. Transient triggering of near and distant earthquakes. *Bull. Seismol. Soc. Am.* 87:294–309

Gomberg J, Bodin P. 1994. Triggering of the Ms = 5.4 Little Skull Mountain, Nevada, earthquake with dynamic strains. *Bull. Seismol. Soc. Am.* 84:844–53

Gomberg J, Bodin P, Larson K, Dragert H. 2004. Earthquake nucleation by transient deformations caused by the M = 7.9 Denali, Alaska, earthquake. *Nature* 427:621–24

Gomberg J, Bodin P, Reasenberg PA. 2003. Observing earthquakes triggered in the near field by dynamic deformations. *Bull. Seismol. Soc. Am.* 93:118–38

Gomberg J, Davis S. 1996. Stress/strain changes and triggered seismicity at The Geysers, California. *J. Geophys. Res.* 101:733–49

Gomberg J, Reasenberg PA, Bodin P, Harris RA. 2001. Earthquake triggering by seismic waves following the Landers and Hector Mine earthquakes. *Nature* 411:462–66

Green HW, Houston H. 1995. The mechanics of deep earthquakes. *Annu. Rev. Earth Planet. Sci.* 23:169–213

Hardebeck JL, Nazareth JJ, Hauksson E. 1998. The static stress change triggering model; constraints from two southern

California aftershock sequences. *J. Geophys. Res.* 103:24427–37

Harris RA, Archuleta RJ, Day SM. 1991. Fault steps and the dynamic rupture process: 2-D numerical simulations of a spontaneously propagating shear fracture. *Geophys. Res. Lett*. 18:893–96

Harris RA, Dolan JF, Hartleb R, Day SM. 2002. The 1999 Izmit, Turkey, earthquake: a 3D dynamic stress transfer model of intraearthquake triggering. *Bull. Seismol. Soc. Am.* 92:245–55

Harris RA, Simpson RW. 1996. In the shadow of 1857: the effect of the great Ft. Tejon earthquake on subsequent earthquakes in southern California. *Geophys. Res. Lett.* 23:229–32

Harris RA, Simpson RW. 1998. Suppression of large earthquakes by stress shadows; a comparison of Coulomb and rate-and-state failure. *J. Geophys. Res.* 103:24439–51

Harris RA, Simpson RW. 2002. The 1999 M_w7.1 Hector Mine, California, earthquake; a test of the stress shadow hypothesis? *Bull. Seismol. Soc. Am.* 92:1497–512

Hauksson E, Jones LM, Hutton K, Eberhart-Phillips D. 1993. The 1992 Landers earthquake sequence: seismological observations. *J. Geophys. Res.* 98:19835–58

Hearn EH, Bürgmann R, Reilinger RE. 2002. Dynamics of Izmit earthquake postseismic deformation and loading of the Duzce earthquake hypocenter. *Bull. Seismol. Soc. Am.* 92:172–93

Hill DP, Johnston MJS, Langbein JO, Bilham R. 1995. Response of Long Valley caldera to the $M_w = 7.3$ Landers, California, earthquake. *J. Geophys. Res.* 100:12985–13005

Hill DP, Reasenberg PA, Michael AJ, Arabasz WJ, Beroza GC. 1993. Seismicity remotely triggered by the magnitude 7.3 Landers, California earthquake. *Science* 260:1617–23

Hodgkinson KM, Stein RS, Marshall G. 1996. The 1954 Rainbow Mountain-Fairview Peak-Dixie Valley earthquake sequences: a triggered normal faulting sequence. *J. Geophys. Res.* 101:25459–72

Hough SE. 2001. Triggered earthquakes and the 1811–1812 New Madrid, central U.S. earthquake sequence. *Bull. Seismol. Soc. Am.* 91:1574–81

Hough SE, Kanamori H. 2002. Source properties of earthquakes near the Salton Sea triggered by the 16 October 1999 M 7.1 Hector Mine, California, earthquake. *Bull. Seismol. Soc. Am.* 92:1281–89

Hough SE, Seeber L, Armbruster JG. 2003. Intraplate triggered earthquakes: observations and interpretations. *Bull. Seismol. Soc. Am.* 93:2212–21

Husen S, Taylor RB, Smith RB, Healser H. 2004. Changes in geyser eruption behavior and remotely triggered seismicity in Yellowstone National Park produced by the 2002 M 7.9 Denali fault earthquake, Alaska. *Geology* 32:537–40

Jaeger JC, Cook NG. 1979. *Fundamentals of Rock Mechanics*. London: Chapman & Hall. 3rd ed.

Jaumé SC, Sykes LR. 1992. Changes in the state of stress on the southern San Andreas fault resulting from the California earthquake sequence of April to June, 1992. *Science* 258:1325–28

Jaumé SC, Sykes LR. 1996. Evolution of moderate seismicity in the San Francisco Bay region, 1850 to 1993: seismicity changes related to the occurrence of large and great earthquakes. *J. Geophys. Res.* 101:765–90

Johnston MJS, Hill DP, Linde AT, Langbein J, Bilham R. 1995. Transient deformation during triggered seismicity from the June 28, 1992, Mw = 7.3 Landers earthquake at Long Valley volcanic caldera, California. *Bull. Seismol. Soc. Am.* 85:787–95

Kagan YY, Jackson DD. 1991. Long-term earthquake clustering. *Geophys. J. Int*. 104: 117–33

Kase Y, Kuge K. 1998. Numerical simulation of spontaneous rupture processes on two noncoplanar faults: the effect of geometry on fault interaction. *Geophys. J. Int.* 135:911–22

Kenner S, Segall P. 1999. Time-dependence of the stress shadowing effect and its relation to the structure of the lower crust. *Geology* 27:119–22

Kilb D, Gomberg J, Bodin P. 2000. Triggering of earthquake aftershocks by dynamic stresses. *Nature* 408:570–74

Kilb D, Gomberg J, Bodin P. 2002. Aftershock triggering by complete Coulomb stress changes. *J. Geophys. Res.* doi:107: 10.1029/2001JB000202

King GCP, Cocco M. 2001. Fault interactions by elastic stress changes: new clues from earthquake sequences. *Adv. Geophys.* 44:1–38

King GCP, Stein RS, Lin J. 1994. Static stress changes and the triggering of earthquakes. *Bull. Seismol. Soc. Am.* 84:935–93

Kirby SH, Kronenberg AK. 1987. Rheology of the lithosphere; selected topics. *Rev. Geophys.* 25:1219–44

Lin J, Stein RS. 2004. Stress interaction in thrust and subduction earthquakes. *J. Geophys. Res.* doi:109:10.1029/2003JB002607

Linde AT, Sacks IS, Johnston MJS, Hill DP, Bilham RG. 1994. Increased pressure from rising bubbles as a mechanism for remotely triggered seismicity. *Nature* 371:408–10

Lynch JC, Bürgmann R, Richards MA, Ferencz RM. 2003. When faults communicate; viscoelastic coupling and earthquake clustering in a simple two-fault system. *Geophys. Res. Lett.* 30:10.1029/2002GL016765

Mallman EP, Zoback MD. 2003. Testing Coulomb stress-transfer models with seismicity rates for the Landers and Kobe earthquakes. *Seismol. Res. Lett.* 75:285

Mathews MV, Reasenberg PA. 1988. Statistical methods for investigating quiescence and other temporal seismicity patterns. *Pure Appl. Geophys*. 126:357–72

Marone C. 1998. Laboratory-derived friction laws and their application to seismic faulting. *Annu. Rev. Earth Planet. Sci*. 26:643–96

Marsan D. 2003. Triggering of seismicity at short timescales following Californian earthquakes. *J. Geophys. Res*. doi: 108:10.1029/2002JB001946

Marsan D, Bean CJ. 2003. Seismicity response to stress perturbations, analyzed for a worldwide catalogue. *Geophys. J. Int.* 154:179–95

Masterlark T, Wang HF. 2002. Transient stress-coupling between the 1992 Landers and 1999 Hector Mine, California, earthquakes. *Bull. Seismol. Soc. Am.* 92:1470–86

Melosh HJ. 1976. Nonlinear stress propagation in the Earth's upper mantle. *J. Geophys. Res*. 81:5621–32

Meltzner AJ, Wald DJ. 2003. Aftershocks and triggered events of the great 1906 California, earthquakes. *Bull. Seismol. Soc. Am.* 93:2160–86

Mohamad R, Darkal AN, Seber D, Sandvol E, Gomez F, Barazangi M. 2000. Remote earthquake triggering along the Dead Sea Fault in Syria following the 1995 Gulf of Aqaba earthquake (Ms = 7.3). *Seismol. Res. Lett.* 71:47–52

Mueller K, Hough SE, Bilham R. 2004. Analysing the 1811-1812 New Madrid earthquakes with recent instrumentally recorded aftershocks. *Nature* 429:284–88

Nalbant SS, Hubert A, King GCP. 1998. Stress coupling between earthquakes in northwest Turkey and the north Aegean Sea. *J. Geophys. Res.* 103:24469–86

Nostro C, Cocco M, Belardinelli ME. 1997. Static stress changes in extensional regimes: an application to southern Apennines (Italy). *Bull. Seismol. Soc. Am.* 87:234–48

Nostro C, Piersanti A, Cocco M. 2001. Normal fault interaction caused by coseismic and postseismic stress changes. *J. Geophys. Res.* 106:19391–410

Oppenheimer DHP, Reasenberg A, Simpson RW. 1988. Fault plane solutions for the 1984 Morgan Hill, California earthquake sequence: Evidence for the state of stress on the Calaveras fault. *J. Geophys. Res.* 93:9007–26

Pankow KL, Arabasz WJ, Pechmann JC, Nava SJ. 2004. Triggered seismicity in Utah from the November 3, 2002, Denali fault earthquake. *Bull. Seismol. Soc. Am*. In press

Parsons T. 2002. Global Omori law decay of triggered earthquakes: Large aftershocks outside the classical aftershock zone. *J. Geophys. Res.* 107:10.1029/2001JB000646

Parsons T, Stein RS, Simpson RW, Reasenberg PA. 1999. Stress sensitivity of fault seismicity: A comparison between limited-offset

oblique and major strike-slip faults. *J. Geophys. Res.* 104:20183–202

Parsons T, Toda S, Stein RS, Barka A, Dieterich JH. 2000. Heightened odds of large earthquakes near Istanbul: An interaction-based probability calculation. *Science* 288:661–65

Peltzer G, Rosen P, Rogez F, Hudnut K. 1998. Poroelastic rebound along the Landers 1992 earthquake surface rupture. *J. Geophys. Res.* 103:30131–45

Pollitz FF, Bürgmann R, Romanowicz B. 1998. Viscosity of oceanic asthenosphere inferred from remote triggering of earthquakes. *Science* 280:1245–49

Pollitz FF, Peltzer G, Bürgmann R. 2000. Mobility of continental mantle: Evidence from postseismic geodetic observations following the 1992 Landers earthquake. *J. Geophys. Res.* 105:8035–54

Pollitz FF, Sacks SI. 1995. Consequences of stress changes following the 1891 Nobi earthquake, Japan. *Bull. Seismol. Soc. Am.* 85:796–807

Pollitz FF, Sacks SI. 1997. The 1995 Kobe, Japan, earthquake; a long-delayed aftershock of the offshore 1944 Tonankai and 1946 Nankaido earthquakes. *Bull. Seismol. Soc. Am.* 87:1–10

Pollitz FF, Sacks SI. 2002. Stress triggering of the 1999 Hector Mine earthquake by transient deformation following the 1992 Landers earthquake. *Bull. Seismol. Soc. Am.* 92:1487–96

Power JA, Moran SC, McNutt SR, Stihler SD, Sanchez JJ. 2001. Seismic response of the Katmai volcanoes to the 6 December 1999 magnitude 7.0 Larluk Lake earthquake, Alaska. *Bull. Seismol. Soc. Am.* 91:57–63

Prejean SG, Hill DP, Brodsky EE, Hough SE, Johnson MJS, et al. 2004. Remotely triggered seismicity on the United States west coast following the M 7.9 Denali fault earthquake. *Bull. Seismol. Soc. Am*. In press

Reasenberg PA, Simpson RW. 1992. Response of regional seismicity to the static stress change produced by the Loma Prieta earthquake. *Science* 255:168790

Reasenberg PA, Simpson RW. 1997. Response of regional seismicity to the static stress change produced by the Loma Prieta earthquake. *U.S. Geol. Surv. Prof. Pap.* 1550-D:49–72

Roeloffs E. 1996. Poroelastic techniques in the study of earthquake-related hydrological phenomena. *Adv. Geophys.* 37:135–95

Roeloffs E, Sneed M, Galloway DL, Sorey ML, Farrar CD, et al. 2003. Water level changes induced by local and distant earthquakes at Long Valley caldera, California. *J. Volc. Geotherm. Res.* 127:269–303

Rydelek PA, Sacks IS. 1999. Large earthquake occurrence affected by small stress changes. *Bull. Seismol. Soc. Am.* 89:822–28

Ruina A. 1983. Slip instability and state variable friction laws. *J. Geophys. Res.* 88: 10359–70

Savage JC, Lisowski M, Prescott WH. 1990. An apparent shear zone trending north-northwest across the Mojave desert into Owens Valley, eastern California. *Geophys. Res. Lett.* 17:2113–16

Scholz CH. 1990. *The Mechanics of Earthquakes and Faulting*. New York: Cambridge Univ. Press. 439 pp.

Scholz CH. 1998. Earthquakes and friction laws. *Nature* 391:37–42

Sieh KE, Stuiver M, Brillinger D. 1989. A more precise chronology of earthquakes produced by the San Andreas Fault in southern California. *J. Geophys. Res.* 94:603–23

Simpson DW. 1986. Triggered earthquakes. *Annu. Rev. Earth Planet. Sci.* 14:21–42

Singh SK, Anderson JG, Rodriguez M. 1998. Triggered seismicity in the Valley of Mexico from major Mexican earthquakes. *Geofis. Int.* 37:3–15

Stark MA, Davis SD. 1996. Remotely triggered microearthquakes at The Geysers geothermal field, California. *Geophys. Res. Lett.* 23:945–48

Stein RS. 1999. The role of stress transfer in earthquake occurrence. *Nature* 402:605–9

Stein RS. 2003. Earthquake conversations. *Sci. Am.* 288:72–79

Stein RS, Barka AA, Dieterich JH. 1997. Progressive failure on the Northern Anatolian

fault since 1939 by earthquake stress triggering. *Geophys. J. Int.* 128:594–604

Stein RS, King GCP, Lin J. 1992. Change in failure stress on the southern San Andreas fault system caused by the 1992 magnitude = 7.4 Landers earthquake. *Science* 258:1328–32

Stein RS, King GCP, Lin J. 1994. Stress triggering of the 1994 M = 6.7 Northridge, California earthquake by its predecessors. *Science* 265:1432–35

Stein RS, Lisowski M. 1983. The 1979 Homestead Valley earthquake sequence, California: Control of aftershocks and postseismic deformation. *J. Geophys. Res.* 88:6477–90

Sturtevant B, Kanamori H, Brodsky EE. 1996. Seismic triggering by rectified diffusion in geothermal systems. *J. Geophys. Res.* 101: 25269–82

Taylor MAJ, Dmowska R, Rice JR. 1998. Upper plate stressing and seismicity in the subduction earthquake cycle. *J. Geophys. Res.* 103:24523–42

Taylor MAJ, Zheng G, Rice JR, Stuart WD, Dmowska R. 1996. Cyclic stressing and seismicity at strongly coupled subduction zones. *J. Geophys. Res.* 101:8363–81

Tibi R, Wiens DA, Inoue H. 2003. Remote triggering of deep earthquakes in the 2002 Tonga sequences. *Nature* 424:921–25

Toda S, Stein RS. 2002. Response of the San Andreas fault to the 1983 Coalinga-Nunez earthquakes: An application of interaction-based probabilities for Parkfield. *J. Geophys. Res.* 107:10.1029/2001JB000172

Toda S, Stein RS. 2003. Toggling of seismicity by the 1997 Kagoshima earthquake couplet: A demonstration of time-dependent stress transfer. *J. Geophys. Res.* 108: 10.1029/2003JB002527

Toda S, Stein RS, Reasonberg PA, Dieterich JH, Yoshida A. 1998. Stress transferred by the 1995 M_w = 6.9 Kobe, Japan, shock: Effect on aftershocks and future earthquake probabilities. *J. Geophys. Res.* 103:24543–65

Townend J, Zoback M. 2000. How faulting keeps the crust strong. *Geology* 28:399–402

Voison C, Campillo M, Ionescu IR, Cotton F, Scotti O. 2000. Dynamic versus static stress triggering and friction parameters: Inferences from the November 23, 1980, Irpinia earthquake. *J. Geophys. Res.* 105:21647–59

Wald DJ, Heaton TH. 1994. Spatial and temporal distribution of slip for the 1992 Landers, California, Earthquake. *Bull. Seismol. Soc. Am.* 84:668–91

Wang WH, Chen CH. 2001. Static stress transferred by the 1999 Chi-Chi, Taiwan, earthquake; effects on the stability of the surrounding fault systems and aftershock triggering with a 3D fault-slip model. *Bull. Seismol. Soc. Am.* 91:1041–52

Weins D. 2001. Seismological constraints on the mechanism of deep earthquakes: Temperature dependence of deep earthquake source parameters. *Phys. Earth Planet. Inter.* 127:145–63

Weins DW, McGuire JJ. 2000. Aftershocks of the March 9, 1994, Tonga earthquake: The strongest known deep aftershock sequence. *J. Geophys. Res.* 105:19067–83

Wyss M, Wiemer S. 2000. Change in the probability for earthquakes in southern California due to the Landers magnitude 7.3 earthquake. *Science* 290:1334–38

Zeng Y. 2001. Viscoelastic stress-triggering of the 1999 Hector Mine earthquake by the 1992 Landers earthquake. *Geophys. Res. Lett.* 28:3007–10

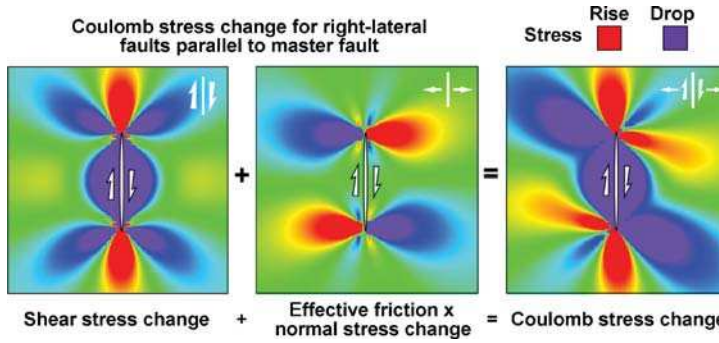

Figure 2 Illustration of a Coulomb stress change calculation (Equation 4). The panels show a map view of a vertical strike-slip fault embedded in an elastic half-space, with imposed slip that tapers toward the fault ends. Stress changes are depicted by graded colors; green represents no change in stress. (From King et al. 1994.)

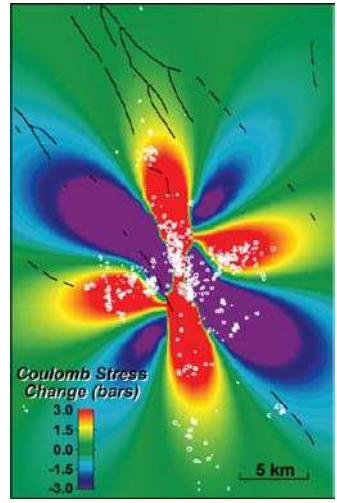

Figure 3 Calculated coseismic Coulomb stress changes and observed aftershocks (*white circles*) associated with 1979 M = 5.5 Homestead Valley, California earthquake. Warm colors (positive) indicate that optimally oriented faults are loaded toward failure and cool colors (negative) indicate that failure is inhibited. Coulomb stresses resolved on optimum right-lateral slip planes for $\mu' = 0.4$. (From King et al. 1994.)

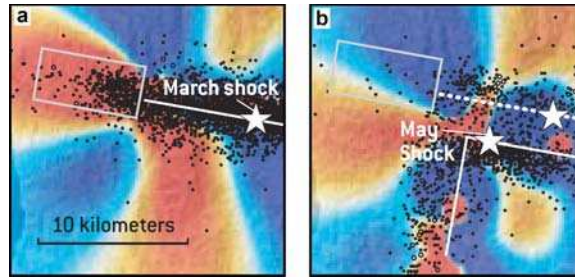

Figure 4 (*a*) A March 1997 earthquake in Kagoshima, Japan increased Coulomb stress and seismicity to the west of the ruptured fault. (*b*) A second earthquake in May decreased stress in that region, leading to a sharp decrease in seismicity. (Modified from Toda & Stein 2003 and Stein 2003.)

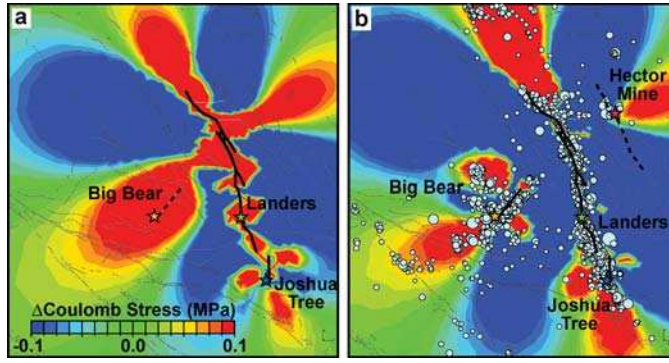

Figure 5 (*a*) The Landers and Joshua Tree earthquakes increased Coulomb stress (*red regions*) where the Big Bear earthquake occurred three hours later. Coulomb stress calculations in (*a*) are for left-lateral strike-slip faults aligned with the Big Bear rupture surface. (*b*) Stress changes induced by the Joshua Tree, Landers, and Big Bear earthquakes increased Coulomb stress in regions where the vast majority of aftershocks occurred over the next seven years, culminating in the 1999 Hector Mine earthquake. Coulomb stress calculations in (*b*) are for right-lateral strike-slip faults aligned with the Hector Mine rupture surface (also reasonable for most aftershocks in the region).

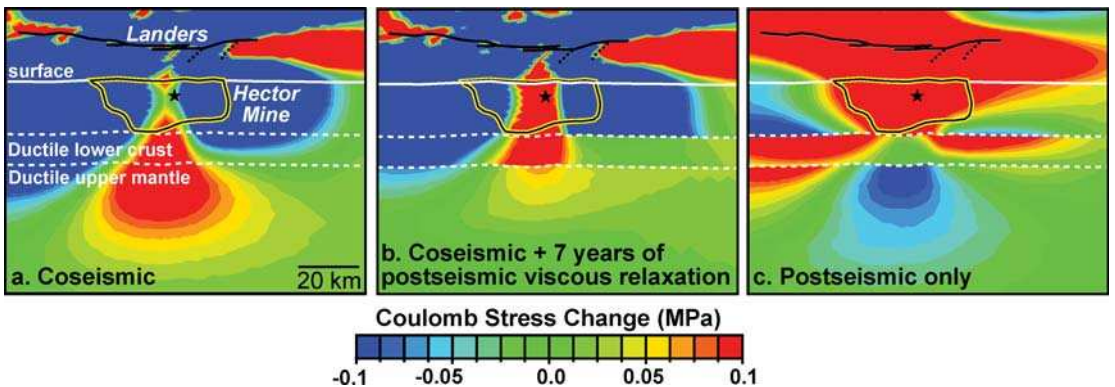

Figure 8 Calculated changes in Coulomb stress along a vertical plane cutting through the Hector Mine rupture surface owing to (*a*) the 1992 Landers earthquake, (*b*) plus stress changes associated with viscous relaxation of the lower crust and upper mantle, and (*c*) owing to viscous processes only. (From Freed & Lin 2001.)

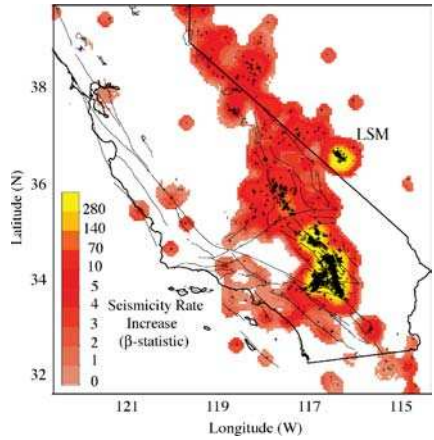

Figure 10 Seismicity rate increases associated with the Landers mainshock. Average increases are quantified with the β-statistic calculated for spatially smoothed (20 km) seismicity ($M \geq 2$). Rate change is calculated for a two-week period immediately after each mainshock, relative to the background period 1987–1992. Plus signs indicate earthquakes in the period after the mainshock. Areas with a β-statistic ≥2.0 are suggestive of a significant average rate increase. White areas represent no catalogued earthquakes in post- and premainshock periods or no detectable rate increases; thin lines represent surface fault traces. A strong increase marked LSM is the (triggered) $M = 5.6$ Little Skull Mountain earthquake and its aftershocks. (From Gomberg et al. 2001.)

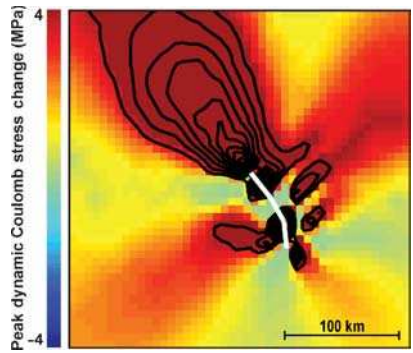

Figure 13 Map at 4.5 km depth of peak dynamic Coulomb stress change with contours indicating levels of stress change ≥4 MPa with equal intervals of 1.5 MPa. Peak dynamic Coulomb stress values are, by definition, always positive. (From Kilb et al. 2002.)

Annual Review of Earth and Planetary Sciences
Volume 33, 2005

CONTENTS

THE EARLY HISTORY OF ATMOSPHERIC OXYGEN: HOMAGE TO ROBERT M. GARRELS, *D.E. Canfield* 1

THE NORTH ANATOLIAN FAULT: A NEW LOOK, *A.M.C. Şengör, Okan Tüysüz, Caner İmren, Mehmet Sakınç, Haluk Eyidoğan, Naci Görür, Xavier Le Pichon, and Claude Rangin* 37

ARE THE ALPS COLLAPSING?, *Jane Selverstone* 113

EARLY CRUSTAL EVOLUTION OF MARS, *Francis Nimmo and Ken Tanaka* 133

REPRESENTING MODEL UNCERTAINTY IN WEATHER AND CLIMATE PREDICTION, *T.N. Palmer, G.J. Shutts, R. Hagedorn, F.J. Doblas-Reyes, T. Jung, and M. Leutbecher* 163

REAL-TIME SEISMOLOGY AND EARTHQUAKE DAMAGE MITIGATION, *Hiroo Kanamori* 195

LAKES BENEATH THE ICE SHEET: THE OCCURRENCE, ANALYSIS, AND FUTURE EXPLORATION OF LAKE VOSTOK AND OTHER ANTARCTIC SUBGLACIAL LAKES, *Martin J. Siegert* 215

SUBGLACIAL PROCESSES, *Garry K.C. Clarke* 247

FEATHERED DINOSAURS, *Mark A. Norell and Xing Xu* 277

MOLECULAR APPROACHES TO MARINE MICROBIAL ECOLOGY AND THE MARINE NITROGEN CYCLE, *Bess B. Ward* 301

EARTHQUAKE TRIGGERING BY STATIC, DYNAMIC, AND POSTSEISMIC STRESS TRANSFER, *Andrew M. Freed* 335

EVOLUTION OF THE CONTINENTAL LITHOSPHERE, *Norman H. Sleep* 369

EVOLUTION OF FISH-SHAPED REPTILES (REPTILIA: ICHTHYOPTERYGIA) IN THEIR PHYSICAL ENVIRONMENTS AND CONSTRAINTS, *Ryosuke Motani* 395

THE EDIACARA BIOTA: NEOPROTEROZOIC ORIGIN OF ANIMALS AND THEIR ECOSYSTEMS, *Guy M. Narbonne* 421

MATHEMATICAL MODELING OF WHOLE-LANDSCAPE EVOLUTION, *Garry Willgoose* 443

VOLCANIC SEISMOLOGY, *Stephen R. McNutt* 461

THE INTERIORS OF GIANT PLANETS: MODELS AND OUTSTANDING QUESTIONS, *Tristan Guillot* 493

THE Hf-W ISOTOPIC SYSTEM AND THE ORIGIN OF THE EARTH AND MOON, *Stein B. Jacobsen* 531

PLANETARY SEISMOLOGY, *Philippe Lognonné* 571

ATMOSPHERIC MOIST CONVECTION, *Bjorn Stevens* 605

OROGRAPHIC PRECIPITATION, *Gerard H. Roe* 645

INDEXES

Subject Index 673

Cumulative Index of Contributing Authors, Volumes 23–33 693

Cumulative Index of Chapter Titles, Volumes 22–33 696

ERRATA

An online log of corrections to *Annual Review of Earth and Planetary Sciences* chapters may be found at http://earth.annualreviews.org